Reaction of cyclopropane, methylcyclopropane, and propylene with hydrogen on the (111) and (110)-(1X2) surfaces of iridium

ARTICLE *in* THE JOURNAL OF PHYSICAL CHEMISTRY · JANUARY 1990

Impact Factor: 2.78 · DOI: 10.1021/j100364a067

3 AUTHORS, INCLUDING:

James R Engstrom
Cornell University
91 PUBLICATIONS **1,915** CITATIONS

Reaction of Cyclopropane, Methylcyclopropane, and Propylene with Hydrogen on the (111) and (110)-(1×2) Surfaces of Iridium

J. R. Engstrom,† D. W. Goodman,*,‡

Surface Science Division, Sandia National Laboratories, Albuquerque, New Mexico 87185

and W. H. Weinberg*,§

Division of Chemistry and Chemical Engineering, California Institute of Technology, Pasadena, California 91125 *(Received: March 13, 1989; In Final Form: July 11, 1989)*

The hydrogenation, isomerization, and hydrogenolysis of cyclopropane, methylcyclopropane, and propylene have been investigated on the (111) and (110)-(1×2) single-crystalline surfaces of iridiium at reactant partial pressures from 0.4 to 10 Torr of hydrocarbon (P_{HC}) and between 20 and 500 Torr of hydrogen (P_{H_2}) and at surface temperatures from 375 to 700 K. Both the kinetics of the reaction (activation energies and preexponential factors) and the dependences of the rates of reaction on the reactant partial pressures (apparent reaction "orders") were examined in detail. Postreaction surface analysis revealed the presence of a carbonaceous residue, the coverage of which was found to vary with the reaction conditions. The reaction of cyclopropane and hydrogen resulted in both hydrogenation to propane and the hydrogenolysis to methane and ethane, with the hydrogenation channel dominating for temperatures below 500 K. The Ir(110)-(1×2) surface was found to be more active than the (111) surface for both the hydrogenation and the hydrogenolysis of cyclopropane. In both cases, the specific activity (per metal surface atom basis) on Ir(110)-(1×2) was greater by a factor between approximately 2 and 10. The hydrogenation of methylcyclopropane on both the Ir(111) and Ir(110)-(1×2) surfaces was found to be dominated by the production of *n*-butane. This result was interpreted qualitatively by invoking parallel reaction mechanisms for the production of *n*-butane and isobutane, with the *n*-butane channel exhibiting a higher apparent activation energy, thus, dominating at the higher temperatures. The hydrogenolysis of methylcyclopropane was found to be similar to that of cyclopropane on both surfaces. However, a selectivity difference was observed between the two surfaces for hydrogenolysis, the product distributions for the major reaction channels were $CH_4 + C_3H_8$ on Ir(111) and $CH_4 + C_2H_6 + C_3H_8$ on Ir(110)-(1×2). The absence of ethane in the major hydrogenolysis channel on the Ir(111) surface can be explained on a stereochemical basis if formation of the appropriate intermediate proceeds through an "edge complex", the formation of which is forbidden sterically on the Ir(111) surface. The Ir(110)-(1×2) surface was found to possess a greater specific activty compared to the Ir(111) surface for the hydrogenation of propylene.

I. Introduction

The reaction of cyclopropane with hydrogen on a variety of transition-metal surfaces has attracted considerable attention since, depending on the reaction conditions, two distinct reaction channels can be observed, namely, "hydrogenation" to form propane and "hydrogenolysis" to form methane and ethane.[1-13] The hydrogenation pathway might be expected to exhibit some similarities to olefin hydrogenation, whereas the hydrogenolysis pathway might resemble alkane hydrogenolysis. Consequently, from an examination of a relatively simple product distribution (methane, ethane, and propane), two (presumably) fundamentally different reaction pathways can be investigated simultaneously. This idealized view of the two classes of reaction of cyclopropane with hydrogen ignores, however, the obvious differences between cyclopropane and both olefins and alkanes. Whereas evidence has been obtained for the existence of a "π-like" nondissociatively adsorbed cyclopropane complex at low temperatures,[14] obviously C–C bond activation (ring-opening) must precede the hydrogenation step. Concerning the hydrogenolysis pathway, unlike alkanes, C–H bond activation in the parent cyclopropane molecule is generally irreversible (and most often preceded by C–C bond activation) as evidenced by the lack of significant exchange between cyclopropane and deuterium over late transition-metal surfaces.[15]

The reaction of cyclopropane with hydrogen has been reported to be slightly "structure sensitive";[11,12] i.e., the activity and/or selectivity have been found to vary with the morphology (dispersion) of the supported metal. For example, on silica-supported nickel catalysts of varying metallic particle size, the activity for both reaction pathways was found to reach a maximum value for crystallites with an average diameter of 12 Å.[12] The *specific* activity (per site basis) for this particle size was approximately a factor of 3 greater than that observed with much larger crystallites of average diameters of ≥50 Å. Similar behavior was reported for both alumina- and silica-supported platinum catalysts.[11] This sensitivity of the specific activity to the structure of the surface for supported catalysts has been corroborated by

† Visiting from the Division of Chemistry and Chemical Engineering, California Institute of Technology, Pasadena, CA 91125. Present address: Department of Chemistry BG-10, University of Washington, Seattle, WA 98195.

‡ Present address: Department of Chemistry, Texas A&M University, College Station, TX 77843.

§ Present address: Department of Chemical Engineering, University of California, Santa Barbara, CA 93106.

(1) Bond, G. C.; Sheridan, J. *Trans. Faraday Soc.* **1952**, *48*, 713.
(2) Bond, G. C.; Turkevich, J. *Trans. Faraday Soc.* **1954**, *50*, 1335.
(3) Addy, J.; Bond, G. C. *Trans. Faraday Soc.* **1957**, *53*, 368; **1957**, *53*, 377; **1957**, *53*, 383; **1957**, *53*, 388.
(4) Bond, G. C.; Newham, J. *Trans. Faraday Soc.* **1960**, *56*, 1501.
(5) Sinfelt, J. H.; Yates, D. J. C.; Taylor, W. F. *J. Phys. Chem.* **1965**, *69*, 1877.
(6) Taylor, W. F.; Yates, D. J. C.; Sinfelt, J. H. *J. Catal.* **1965**, *4*, 374.
(7) Dalla Betta, R. A.; Cusumano, J. A.; Sinfelt, J. H. *J. Catal.* **1970**, *19*, 343.
(8) Anderson, J. R.; Avery, N. R. *J. Catal.* **1967**, *8*, 48.
(9) Chevreau, T.; Gault, F. G. *J. Catal.* **1977**, *50*, 124.
(10) Maire, G.; Plouidy, G.; Prudhomme, J. C.; Gault, F. G. *J. Catal.* **1965**, *4*, 556.
(11) Coenen, J. W. E.; Schats, W. M. T. M.; van Meerten, R. Z. C. *Bull. Soc. Chim. Belg.* **1979**, *88*, 435.
(12) Boudart, M.; Aldag, A.; Benson, J. E.; Dougharty, N. A.; Harkins, C. G. *J. Catal.* **1966**, *6*, 92.
(13) Goodman, D. W. *J. Vac. Sci. Technol.* **1984**, *A2*, 873.
(14) Hoffmann, F. M.; Felter, T. E.; Weinberg, W. H. *J. Chem. Phys.* **1982**, *76*, 3799. Felter, T. E.; Hoffmann, F. M.; Thiel, P. A.; Weinberg, W. H. *Surf. Sci.* **1983**, *130*, 163.

(15) Deuteriocyclopropanes have been observed from the exchange of cyclopropane and deuterium on tungsten films at temperatures near 275 K.[8] In fact, deuteriocyclopropanes were the *major* reaction products in this case. Deuterium exchange with the parent hydrocarbon has also been reported on supported rhodium, iridium, and platinum catalysts at temperatures near 375 K.[3] Compared to both the tungsten films[8] and the corresponding rates of propane production on these supported catalysts, the rates of exchange were considerably less on these group VIII metals, e.g., approximately 1% of the rate of propane production at 375 K.

0022-3654/90/2094-0396$02.50/0

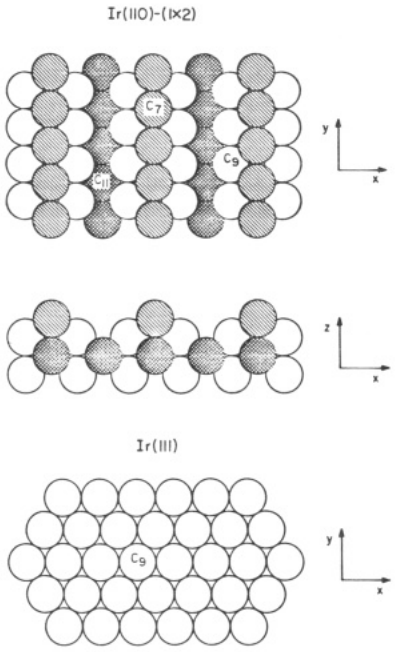

Figure 1. Structures of the (110)-(1×2) and (111) surfaces of iridium. The z axis is perpendicular to the plane of the surface. The C_n designate the coordination numbers of the metal surface atoms.[17]

more recent work by Goodman[13] on oriented single-crystalline surfaces of nickel.

We have undertaken a fundamental examination of the role of surface structure in the reaction of cyclopropane with hydrogen on two different orientations of iridium single crystals, namely, the close-packed (111) and the corrugated (110)-(1×2) surfaces (cf. Figure 1). Primarily, we present here measurements of the reaction kinetics coupled with postreaction surface characterization via Auger electron spectroscopy. The clean Ir(110)-(1×2) surface reconstructs into a (1×2) superstructure,[16] which contains a large fraction (25%) of low-coordination-number [C_7[17]] edge atoms, whereas a perfect (111) surface contains no such atoms. The (1×2) reconstruction is expected to be stable *under reaction conditions*, i.e., in the presence of adsorbed hydrocarbon residues and/or surface carbon and hydrogen.[18-21]

We have considered also the reaction of both methylcyclopropane and propylene with hydrogen on these two surfaces of iridium. The study of methylcyclopropane provides a more detailed picture of the reaction mechanisms. For example, by examining the relative rates of *n*-butane and isobutane production as a function of reaction conditions, particular adsorbed intermediates of the hydrogenation reaction are suggested. On the other hand, the selectivity for the production of methane and propane versus (two molecules of) ethane suggests intermediates relevant to the hydrogenolysis reaction. Finally, the study of the hydrogenation of propylene is useful for a more complete understanding of the mechanism of the hydrogenation reaction of cyclopropane. For example, if both propylene and propane are produced from a common intermediate in the reaction of cyclopropane, a comparison to propylene hydrogenation may implicate the nature of the rate-limiting step (or steps); e.g., the rate-limiting step could involve either the rate of formation of this intermediate or the rate at which the intermediate is hydrogenated.

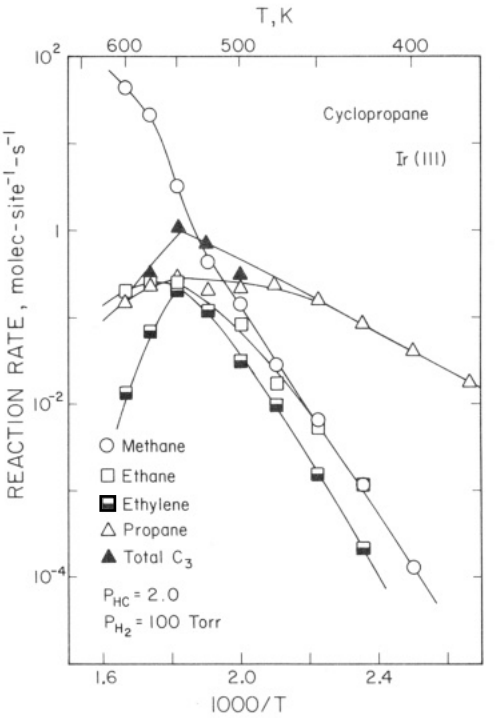

Figure 2. Specific reaction rates (*product* molecules·site^{-1}·s^{-1}) for the reaction of cyclopropane and hydrogen on the Ir(111) surface. The partial pressure of cyclopropane was 2.0 Torr, whereas that of hydrogen was 100 Torr.

II. Experimental Procedures

The experiments reported here were performed in a high-pressure stainless steel reaction chamber (total volume $\simeq$ 600 cm^3) linked to an ultrahigh-vacuum (UHV) analysis chamber, similar to that described previously.[22] The chambers, which are pumped separately, are connected by a metal valve, and the base pressure in both is 10^{-10} Torr. Facilities are available in the UHV analysis chamber for Auger electron spectroscopy, ion sputtering, and quadrupole mass spectrometry (UTI 100C). The catalyst samples are attached to a long-throw retraction bellows and can be translated vertically to various positions in either chamber. The single-crystalline catalysts of iridium (total surface area, $\simeq$1 cm^2) were mounted on tungsten wire leads and were heated resistively. The temperature was controlled manually and was measured with a W/5% Re–W/26% Re thermocouple spot-welded to the crystal. The crystals were cleaned in the UHV analysis chamber by argon ion sputtering, heating in 5×10^{-7} Torr of oxygen at 700 K and annealing to 1600 K. Surface cleanliness was verified by Auger electron spectroscopy.

The cyclopropane (99.0%) and propylene (99.6%) employed in these experiments were research purity from Matheson. The methylcyclopropane was ultrahigh purity (99.95%) from API Standard Reference Materials. The hydrogen was ultrahigh purity (99.999%). The hydrocarbons were purified further by degassing at 80 K, followed by triple distillation from a liquid pentane/solid pentane bath. Reaction products were detected by gas chromatography (GC), which, in this case, is superior to mass spectrometric detection (e.g., there are no complications due to the interpretation of fragmentation patterns). Absolute reaction rates (molecules·cm^{-2}·s^{-1}) were calculated by utilizing the measured volume of the reactor, the time of reaction (batch reactor kinetics), and the measured geometrical surface areas of the crystals. Specific rates (molecules·site^{-1}·s^{-1}) were calculated by using substrate densities of 1.57×10^{15} and 1.93×10^{15} cm^{-2} for the (111) and (110)-(1×2) surfaces, respectively. The corresponding saturation coverages of hydrogen, commonly used to determine metallic surface areas of supported catalysts, are within ap-

(16) Chan, C.-M.; Van Hove, M. A.; Weinberg, W. H.; Williams, E. D. *Solid State Commun.* **1979**, *30*, 47. Chan, C.-M.; Van Hove, M. A.; Weinberg, W. H.; Williams, E. D. *Surf. Sci.* **1980**, *91*, 430.
(17) van Hardeveld, R.; Hartog, F. *Adv. Catal.* **1972**, *22*, 75.
(18) Wittrig, T. S.; Szuromi, P. D.; Weinberg, W. H. *J. Chem. Phys.* **1982**, *76*, 716.
(19) Wittrig, T. S.; Szuromi, P. D.; Weinberg, W. H. *Surf. Sci.* **1982**, *116*, 414.
(20) Szuromi, P. D.; Engstrom, J. R.; Weinberg, W. H. *J. Chem. Phys.* **1984**, *80*, 508.
(21) Weinberg, W. H. In *Survey of Progress in Chemistry*; Academic: New York, 1983; Vol. 10, p 1.
(22) Goodman, D. W.; Kelley, R. D.; Madey, T. E.; Yates, J. T., Jr. *J. Catal.* **1980**, *63*, 226. Goodman, D. W. *Acc. Chem. Res.* **1984**, *17*, 194.

TABLE I: Carbonaceous Residues following Reactions[a]

reactant	fractional carbon coverage, θ_C
Ir(111) Surface	
cyclopropane	0.48 ± 0.08
methylcyclopropane	0.52 ± 0.10
Ir(110)-(1×2) Surface	
cyclopropane	0.49 ± 0.11
methylcyclopropane	0.54 ± 0.09

[a] For P_{H_2} = 100 Torr, P_{HC} = 2 Torr, and T = 375–700 K.

proximately 20% of these substrate densities in each case.[23,24] However, it should be noted that if, for example, either the low-coordination-number (C_7) or the high-coordination-number (C_{11}) surface atoms provide the only "active sites" for a particular reaction (cf. Figure 1), then this normalization will *under*estimate the specific rate for the Ir(110)-(1×2) surface by a factor of 4.

III. Results

A. Cyclopropane. 1. Ir(111) Surface. Specific rates (product molecules·site^{-1}·s^{-1}) of the reaction of cyclopropane with hydrogen on the Ir(111) surface are shown in Figure 2, plotted in an Arrhenius form. The specific procedure in each case involved the following: retracting the catalyst into the reaction chamber, filling the chamber with the reactants to the desired partial pressure, heating the catalyst to the desired temperature for the specific time period, cooling the catalyst to room temperature, pumping out the reactant/product mixture for analysis via GC, and returning the catalyst to the UHV chamber for analysis via Auger electron spectroscopy. These data represent steady-state reaction rates, as verified by measuring the total amount of product formed after various times of reaction, typically 50–2000 s, depending on the temperature. No induction periods were detected; i.e., the steady-states were achieved in reaction times ≪50 s. To avoid secondary reactions and maintain approximately constant reactant partial pressures, conversions were restricted typically to below 1%. The "standard" reactant partial pressure ratio, P_{H_2}/P_{HC}, was 100/2, with a cyclopropane pressure of 2.0 Torr.

Postreaction surface characterization by Auger electron spectroscopy indicated the presence of a *submonolayer* carbonaceous residue, the fractional coverage of which was essentially independent of temperature (T = 375–600 K) for these reactant partial pressures. The measured value of the fractional coverage of carbon on the surface is given in Table I. Postreaction thermal desorption of the surface containing the carbonaceous residue produced only H_2, which gave a broad desorption feature from approximately 350 to 800 K, the dominant feature exhibiting a peak temperature of approximately 500 K (see text below and Figure 7). No attempts were made to determine the average stoichiometry (C_xH_y) of this carbonaceous residue, since it is *not* representative of the relevant adsorbed reaction intermediates under reaction conditions. This was demonstrated by returning the catalyst to the reaction chamber (after the reactants had been pumped away, maintaining the catalyst at room temperature) and reacting the carbonaceous residue with pure hydrogen at the relevant reaction temperatures. Methane was the only reaction product observed in all cases; i.e., no C_2 or C_3 products were produced. Moreover, the measured rate of methane production from this titration procedure was at least a factor of 10 smaller than that observed in the presure of 2 Torr of cyclopropane.

As may be seen in Figure 2, the only reaction products obseved were methane, ethane, ethylene, propane, and propylene (total C_3 product refers to propane and propylene). The two major reaction channels at low temperatures ($T \lesssim 450$ K) are given by

$$c\text{-}C_3H_6 + H_2 \rightarrow C_3H_8$$

i.e., the (dominant) hydrogenation pathway, and

$$c\text{-}C_3H_6 + 2H_2 \rightarrow CH_4 + C_2H_6$$

(23) Ibbotson, D. E.; Wittrig, T. S.; Weinberg, W. H. *J. Chem. Phys.* **1980**, *72*, 4885.
(24) Engstrom, J. R.; Tsai, W.; Weinberg, W. H. *J. Chem. Phys.* **1987**, *87*, 3104.

TABLE II: Apparent Rate Parameters[a] from the Ir(111) Surface

temp range, K	R(450 K),[b] molecules·site^{-1}·s^{-1}	$k_{app}^{(0)}$, molecules·site^{-1}·s^{-1}	E_{app}, kcal·mol^{-1}
	$c\text{-}C_3H_6 + H_2 \rightarrow C_3H_8$		
375–450	0.16	$1.0 \times 10^{3\pm0.5}$	9.9 ± 1
	$c\text{-}C_3H_6 + 2H_2 \rightarrow CH_4 + C_2H_6\ (+C_2H_4)$		
400–500	6.8×10^{-3}	$5.4 \times 10^{10\pm1}$	26.6 ± 2
	$c\text{-}C_3H_5CH_3 + H_2 \rightarrow n\text{-}C_4H_{10}\ (+n\text{-}C_4H_8)$		
375–475	0.92	$3.9 \times 10^{6\pm0.5}$	13.6 ± 1
	$c\text{-}C_3H_5CH_3 + 2H_2 \rightarrow CH_4 + C_3H_8\ (+C_3H_6)$		
375–450	1.1×10^{-2}	$6.6 \times 10^{7\pm1}$	20.4 ± 2
	$C_3H_6 + H_2 \rightarrow C_3H_8$		
425–600	1.0	$0.8 \times 10^{0\pm1}$	−0.2 ± 2
	$C_3H_6 + 2H_2 \rightarrow CH_4 + C_2H_6\ (+C_2H_4)$		
400–500	5.6×10^{-3}	$1.5 \times 10^{9\pm1}$	23.8 ± 2

[a] Rate parameters were fit to the total conversion within the specified temperature range by utilizing the expression $R = k_{app}^{(0)} \exp(-E_{app}/k_BT)$. Reactant partial pressures were 2.0 Torr of hydrocarbon and 100 Torr of hydrogen. [b] Reaction rate is in terms of total conversion.

i.e., the hydrogenolysis pathway. The similarities of the temperature dependence of the reaction rates suggest that the production of ethylene is associated with the hydrogenolysis pathway. It is immediately evident from Figure 2 that the apparent activation energy for the production of propane is much lower than that for the production of methane and ethane (and ethylene). In addition, for $T \lesssim 450$ K, the rate of hydrogenation exceeds that of hydrogenolysis by at least 1 order of magnitude. Extrapolating these rates to lower temperatures clarifies why the hydrogenolysis reaction was not observed on supported iridium catalysts at lower temperatures ($T \leq 375$ K).[4,7] The apparent kinetic rate parameters obtained from the data shown in Figure 2 (for $T \leq 450$–500 K) are given in Table II for the two major reaction channels. The apparent activation energy of 9.9 ± 1 kcal·mol^{-1} observed here for the hydrogenation of cyclopropane agrees well with previous work on supported iridium catalysts, where values of 9.8–11.5[3,4] and 13 kcal·mol^{-1} [7] were obtained. Extrapolating the data of Sinfelt and co-workers,[4] obtained on a 10 wt % Ir silica-supported catalyst, to our reactant partial pressures and a temperature of 375 K, the predicted specific rate of hydrogenation (to propane) is 0.05 molecules·site^{-1}·s^{-1}, which is in good agreement with the value of 0.017 molecules·site^{-1}·s^{-1} measured here on Ir(111).

As the temperature is increased above approximately 475 K, a number of changes in the reaction product distribution are observed. Whereas linear Arrhenius behavior is apparent with respect to the *total* C_3 production for temperatures up to approximately 550 K, the selectivity for propylene increases with increasing temperature. The linear Arrhenius behavior suggests that propylene and propane are formed from a common intermediate, whereas the increase in propylene ($T \lesssim 550$ K) production is best explained by a depletion in the steady-state coverage of hydrogen adatoms with increasing temperature. Above temperatures of approximately 500 K, the relative production of ethane and ethylene decreases, while the production of methane increases. The change in the selectivity of the hydrogenolysis pathway (i.e., $3CH_4$ vs $CH_4 + C_2H_6$) is *not* accompanied, however, by any change in the apparent reaction kinetics. This is evident in Figure 3, where the total rate of hydrogenolysis is plotted in an Arrhenius form in terms of *cyclopropane conversion to C_1 and C_2 products*. In particular, a least-squares fit of the data shown in Figure 3 results in, within experimental error, apparent rate parameters identical with those given in Table II (which were fit to $T \leq 500$ K); namely, $k_{app}^{(0)} \simeq 1.1 \times 10^{11\pm1}$ molecules·site^{-1}·s^{-1} and $E_{app} \simeq 27.3 \pm 2$ kcal·mol^{-1}. This observation is unlike that found for alkane hydrogenolysis, where concomitant with the increase in the selectivity for methane, a change was also observed in the apparent reaction kinetics.[25] *Thus, for cyclopropane, the rate-*

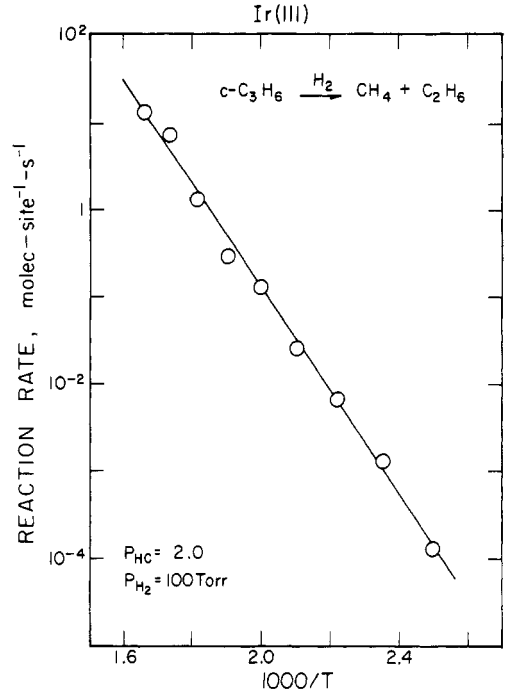

Figure 3. Specific rates of hydrogenolysis of cyclopropane on the Ir(111) surface, plotted in terms of cyclopropane conversion to methane, ethane, and ethylene. Hydrogenolysis conversion is equivalent to $^1/_3R_{C_1} + {}^2/_3R_{C_2}$. The partial pressure of cyclopropane was 2.0 Torr, and that of hydrogen was 100 Torr.

limiting step (or steps) of the hydrogenolysis reaction does not vary for temperatures between 400 and 600 K at these reactant partial pressures.

The dependence of the specific rates of reaction on the reactant partial pressures has been examined at two different temperatures. Data are shown in Figure 4 where reaction rates were measured for variations in both the hydrogen and cyclopropane partial pressures, while maintaining a constant partial pressure of the other and a constant temperature of 450 K. This temperature corresponds to the onset of a detectable rate of propylene production (cf. Figure 2). As may be seen in Figure 4, with the possible exception of the data given by P_{HC} = 2.0 Torr and P_{H_2} = 20 Torr, both decreasing the hydrogen partial pressure and increasing the hydrocarbon partial pressure lead to an increase in the rate of propylene production. Similar behavior is observed for the hydrogenolysis pathway insofar as the rate of ethylene production is concerned. These observations are consistent with a reaction mechanism in which hydrogen and cyclopropane effectively compete for the "same" adsorption sites; i.e., hydrogen adatoms can block the dissociative adsorption of cyclopropane and vice versa. Thus, increasing the temperature, decreasing the hydrogen partial pressure, and increasing the cyclopropane partial pressure all act to deplete the steady-state coverage of hydrogen adatoms and, hence, shift the selectivity to the more dehydrogenated products, propylene and ethylene.

The apparent reaction "order" in P_{HC}, $(\partial \ln R/\partial \ln P_{HC})_{T,P_{H_2}}$, for the hydrogenation/isomerization pathway (i.e., *total* C_3 production) is approximately unity for cyclopropane partial pressures below 2.0 Torr and decreases somewhat at higher pressures for T = 450 K and P_{H_2} = 100 Torr. A *maximum* is observed with respect to the hydrogen partial pressure, the apparent order decreasing from $\sim$1 to $\sim -^1/_2$ as P_{H_2} is increased for T = 450 K and P_{HC} = 2.0 Torr. A maximum in the rate of production of propane as a function of the hydrogen partial pressure for the reaction of cyclopropane and hydrogen has been observed previously on supported iridium catalysts,[4] consistent with our observations here. The $-^1/_2$ order in P_{H_2} for hydrogen

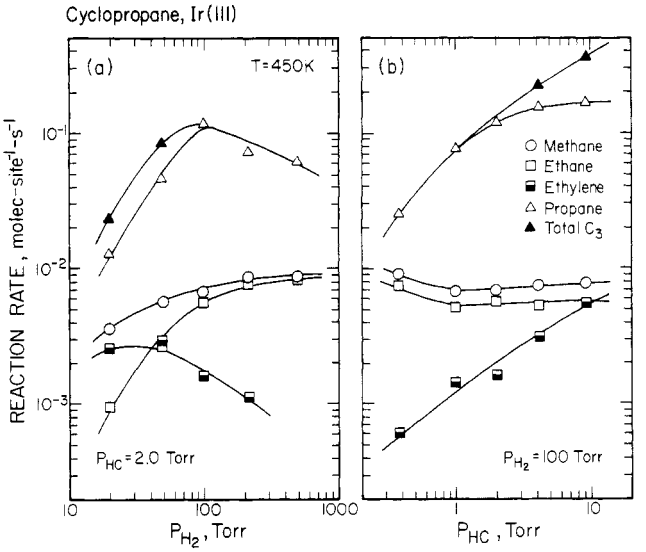

Figure 4. Specific reaction rates for the reaction of cyclopropane and hydrogen on the Ir(111) surface at a temperature of 450 K. (a) The partial pressure of cyclopropane was maintained at 2.0 Torr as the partial pressure of hydrogen was varied. (b) The partial pressure of hydrogen was maintained at 100 Torr as the partial pressure of cyclopropane was varied.

partial pressures above 100 Torr is consistent with a mechanism involving competition between the reactants for adsorption sites; i.e., hydrogen is acting to block the adsorption of cyclopropane. The positive order in P_{H_2} for pressures below 100 Torr suggests that the hydrogenation step is not rapid with respect to the overall rate of reaction. Similarly, since the *total* rate of C_3 production is a positive order in P_{H_2} in this pressure regime, if propane and propylene are formed from a common intermediate, it may be more dehydrogenated than propylene (e.g., a C_3H_5(a) adsorbed species).

Alternatively, the positive order in P_{H_2} could involve accelerated removal of a "soft" carbonaceous residue by adsorbed hydrogen atoms, i.e., this residue acting to deplete the active surface area of the catalyst. We believe, however, that this is unlikely for the following reason. As discussed above, the adsorbed hydrogen concentration is depleted by both decreasing P_{H_2} and increasing P_{HC}. Thus, the coverage of a soft carbonaceous residue would be expected to increase with increasing P_{HC}, which would lead to a negative order in P_{HC}. As may be seen in Figure 4, negative reaction orders in P_{HC} are not observed for either reaction channel.

In contrast to the hydrogenation pathway, the total rate of hydrogenolysis (i.e., total conversion of cyclopropane to methane, ethane, and ethylene) is only weakly dependent on the reactant partial pressures at T = 450 K. The apparent order with respect to P_{HC} is essentially zero, whereas that with respect to P_{H_2} is nearly zero for $P_{H_2} \geq$ 100 Torr and exhibits a small positive value for $P_{H_2} <$ 100 Torr. These observations should be contrasted with those found for propane hydrogenolysis,[25] where, for $T \lesssim$ 500 K, the reaction rates are approximately first order in hydrocarbon partial pressure and large negative order ($\lesssim -^1/_2$) in hydrogen partial pressure. The orders for alkane hydrogenolysis can be rationalized in terms of a pseudoequilibrium between the gas-phase hydrocarbon and hydrogen and an adsorbed, dehydrogenated parent hydrocarbon fragment and hydrogen adatoms.[25] The behavior of the hydrogenolysis pathway observed here suggests that this pseudoequilibrium does not occur for cyclopropane. *Rather, formation of the appropriate reaction intermediate is irreversible for cyclopropane.*

The sensitivity of the specific rates of reaction on the reactant partial pressures is considerably different at higher temperatures where dramatic changes in the selectivity are observed (cf. Figure 2). This is reflected in the data that are shown in Figure 5, which were measured at a temperature of 575 K. We shall emphasize here the most notable feature of the data shown in Figure 5, i.e., the dramatic shift in the selectivity that is observed for P_{H_2}/P_{HC}

(25) Engstrom, J. R.; Goodman, D. W.; Weinberg, W. H. *J. Am. Chem. Soc.* **1988**, *110*, 8305.

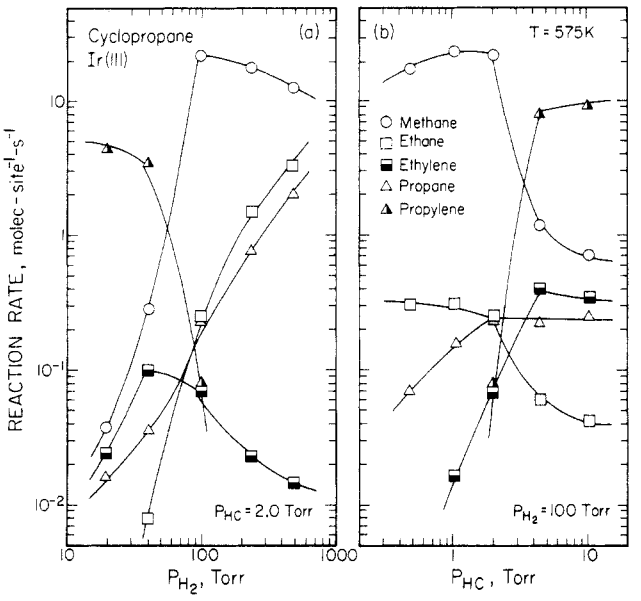

Figure 5. Specific reaction rates for the reaction of cyclopropane and hydrogen on the Ir(111) surface at a temperature of 575 K. (a) The partial pressure of cyclopropane was maintained at 2.0 Torr as the partial pressure of hydrogen was varied. (b) The partial pressure of hydrogen was maintained at 100 Torr as the partial pressure of cyclopropane was varied.

< 50. This virtual step-function change in the selectivity from methane (hydrogenolysis) to propylene (isomerization) is accompanied by and probably a consequence of a nearly irreversible transformation in the coverage and/or structure of the carbonaceous residue. Postreaction surface characterization by Auger electron spectroscopy indicates that the fractional carbon coverage increases from a value of $\theta_C \simeq 0.46 \pm 0.1$ to values of $\theta_C \simeq 0.8$–1.0 ± 0.1, as P_{H_2}/P_{HC} is reduced below a value of 50 at a temperature of 575 K. The specific values for the carbon coverage corresponding to the reaction conditions given by Figure 5 are shown in Figure 6b. The data of Figure 5 are also shown in Figure 6a where they are plotted in terms of a hydrogenation/isomerization (C_3) selectivity and a hydrogenolysis (C_1 and C_2) selectivity. Clearly, the hydrogenolysis pathway dominates on the "low"-carbon-coverage surface ($\theta_C \simeq 0.46$), whereas the hydrogenation/isomerization pathway dominates on the highly carburized surface ($\theta_C \simeq 0.8$–1.0).

The cause of the selectivity shift may be understood better by considering the nature of the highly carburized surface. The high-carbon-coverage residue is considerably less reactive to gas-phase hydrogen than the low-coverage residue. For example, reaction of the residue corresponding to $\theta_C \simeq 0.96$ of Figure 6 with pure hydrogen (~100 Torr) for 300 s at 575 K reduced the carbon coverage by only 10%, whereas a similar treatment of the low-coverage residue produces essentially a clean surface. In addition, postreaction thermal desorption from the high-coverage residue (monitoring H_2, the only observed desorption product) shows that it contains less hydrogen compared to the low-coverage residue. Thermal desorption spectra representative of the low- and high-coverage residues are shown in Figure 7. It is important to realize that the *majority* of the hydrogen desorbing in these spectra is a result of C–H bond cleavage. In particular, previous work examining H_2 on the clean Ir(111) surface[24] indicates that the coverage of irreversibly bound hydrogen adatoms at 300 K is less than 0.1 monolayers. This hydrogen bound to the Ir metal surface desorbs completely by 400 K. Integration of the spectra shown in Figure 7 indicates that on a per-carbon-atom basis, the high-coverage residue contains approximately one-third of the hydrogen evolved from the low-coverage residue. This result suggests the high-coverage residue is extensively dehydrogenated with virtually all of the carbon atoms bound strongly to the surface.

The lower hydrogen content of the carbonaceous residue and its lower reactivity toward the hydrogen suggest that C–C bonds

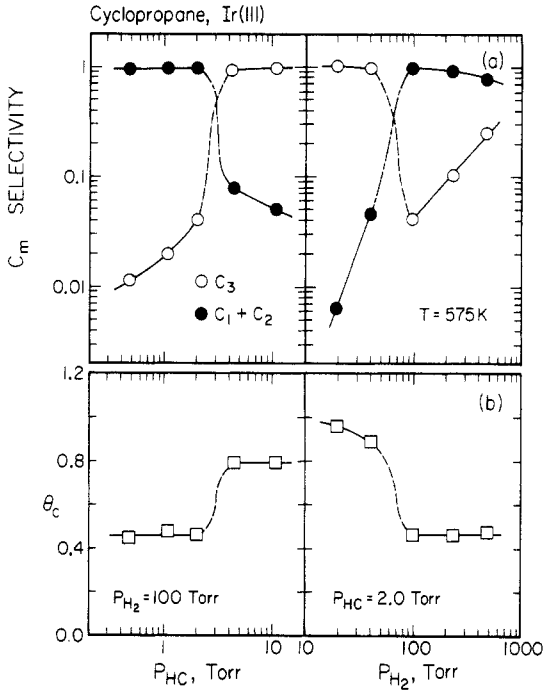

Figure 6. (a) Relative selectivity for hydrogenation/isomerization (C_3) and hydrogenolysis ($C_1 + C_2$) from the reaction of cyclopropane and hydrogen on the Ir(111) surface at a temperature of 575 K. The reaction conditions are identical with those given in Figure 5. (b) The fractional surface coverage of the carbonaceous residue at the corresponding reaction conditions. The experimental uncertainty in the measurement of the coverage of the carbonaceous residue is approximately ±0.1 monolayer.

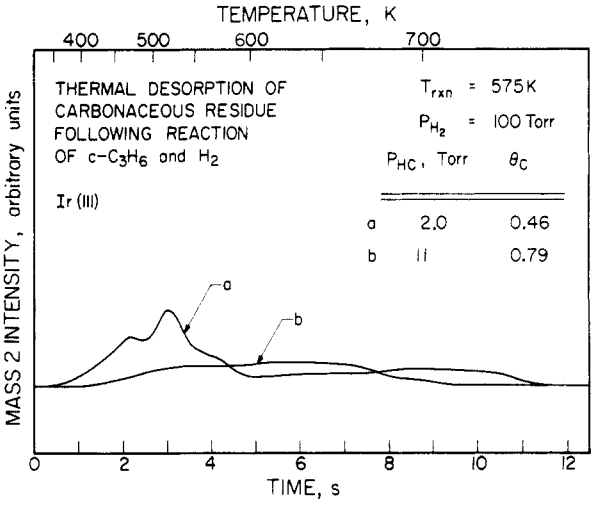

Figure 7. Thermal desorption spectra of H_2 from the carbonaceous residue following the reaction of cyclopropane and hydrogen on the Ir-(111) surface at the conditions indicated.

may be present in the high-coverage carbonaceous residue. However, we do not believe the formation of graphite is significant under these reaction conditions. For example, the density of carbon atoms on the basal plane of graphite is equal to 3.81×10^{15} atoms·cm^{-2}, which would correspond to a fractional coverage of 2.43 monolayers on the Ir(111) surface. Thus, if graphite were formed at a mean coverage of 1.0 monolayers, it would exist in islands covering 41% of the Ir(111) surface. The most probable effect of this graphite overlayer on the reaction kinetics would be a reduction in the specific activity by a factor of 0.41; i.e., a variation in *selectivity* would be difficult to reconcile. Consequently, we submit that the high-coverage carbonaceous residue (i.e., $\theta_C \simeq 0.8$–1.0) is most likely an uniformly dispersed adlayer consisting of carbon atoms and/or partially dissociated hydrocarbon fragments.

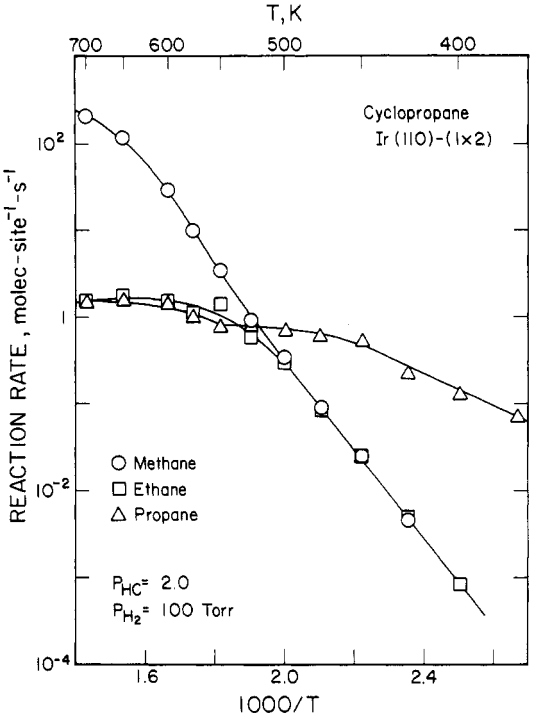

Figure 8. Specific reaction rates for the reaction of cyclopropane and hydrogen on the Ir(110)-(1×2) surface. The partial pressure of cyclopropane was 2.0 Torr, whereas that of hydrogen was 100 Torr.

The strongly bound carbonaceous residue, approaching one monolayer in coverage, can be expected to perturb appreciably the ability of the metal surface to bind the relevant reaction intermediates. Although the carburized surface can be expected to lead to a lower steady-state concentration of hydrogen adatoms and, hence, an increase in the relative amount of unsaturated products (propylene), the proper explanation is not that simple. If the hydrogen adatom concentration is the sole cause of the observed behavior, then the selectivity shift should be from propylene to *propane* as P_{H_2} is increased. However, since the selectivity shift is to *methane* (hydrogenolysis), the implication is that *either the structure or the binding energy of the adsorbed hydrocarbon intermediate is changed significantly on the carburized surface.*

The dramatic shift in the selectivity from hydrogenolysis to isomerization, due in this case to "self-poisoning" of the metal surface by the reactants, has been observed previously. For the reaction of cyclopropane and hydrogen on a Ni(111) surface under similar conditions (P_{HC} = 1.0 Torr, P_{H_2} = 100 Torr, and T = 550 K), Goodman[13] observed a selectivity shift of similar magnitude upon the addition of $^1/_3$ of a monolayer of sulfur.

2. Ir(110)-(1×2) Surface. Specific rates of the reaction of cyclopropane with hydrogen on the Ir(110)-(1×2) surface are shown in Figure 8, plotted in an Arrhenius form. These data represent steady-state reaction rates, obtained for conversions that were restricted typically to below 1%. The "standard" reactant partial pressure ratio, P_{H_2}/P_{HC}, was 100/2, with a cyclopropane partial pressure of 2.0 Torr.

Postreaction surface characterization by Auger electron spectroscopy indicated the presence of a submonolayer carbonaceous residue on the Ir(110)-(1×2) surface. The measured value of the fractional coverage, which was essentially independent of temperature for these reactant partial pressures, is given in Table I. The fractional coverages of carbon observed on both surfaces of iridium for the reaction of cyclopropane and hydrogen are identical with one another. This tends to rule out the possibility that sites unique to the (110)-(1×2) surface are being poisoned selectively. Furthermore, postreaction thermal desorption from the carbonaceous overlayer produced only H_2, and the resulting desorption spectra were similar to those observed from the (111) surface (cf. Figure 7, spectrum a). Reaction of the carbonaceous overlayer with hydrogen produced only methane in all cases.

TABLE III: Apparent Rate Parameters[a] from the Ir(110)-(1×2) Surface

temp range, K	R(450 K),[b] molecule·site^{-1}·s^{-1}	$k_{app}^{(0)}$, molecule·site^{-1}·s^{-1}	E_{app}, kcal·mol^{-1}
	$c\text{-}C_3H_6 + H_2 \rightarrow C_3H_8$		
375–450	0.54	$7.8 \times 10^{3\pm0.5}$	8.7 ± 1
	$c\text{-}C_3H_6 + 2H_2 \rightarrow CH_4 + C_2H_6$		
400–525	2.5×10^{-2}	$3.0 \times 10^{9\pm1}$	23.0 ± 2
	$c\text{-}C_3H_5CH_3 + H_2 \rightarrow n\text{-}C_4H_{10}$ (+n-C_4H_8)		
375–475	3.6	$2.2 \times 10^{7\pm0.5}$	14.2 ± 1
	$c\text{-}C_3H_5CH_3 + 2H_2 \rightarrow CH_4 + C_2H_6 + C_3H_8$		
375–475	1.3×10^{-2}	$1.3 \times 10^{7\pm1}$	18.6 ± 2
	$C_3H_6 + H_2 \rightarrow C_3H_8$		
450–600	14	$0.2 \times 10^{0\pm1}$	−3.6 ± 2
	$C_3H_6 + 2H_2 \rightarrow CH_4 + C_2H_6$ (+C_2H_4)		
400–450	1.7×10^{-2}	$9.3 \times 10^{10\pm1}$	26.3 ± 2

[a] Rate parameters were fit to the total conversion within the specified temperature range by utilizing the expression $R = k_{app}^{(0)} \exp(-E_{app}/k_BT)$. Reactant partial pressures were 2.0 Torr of hydrocarbon and 100 Torr of hydrogen. [b] Reaction rate is in terms of total conversion.

The only reaction products observed on the Ir(110)-(1×2) surface were methane, ethane, and propane. In particular, no unsaturated hydrocarbons (e.g., ethylene or propylene) were produced, in contrast to the observations on the Ir(111) surface. As on Ir(111), the product distribution is described by two major reaction channels for temperatures below approximately 500 K: the hydrogenation pathway to form propane and the hydrogenolysis pathway to form methane and ethane. The apparent rate parameters obtained from the data shown in Figure 8 (for $T \leq$ 475 K) are given in Table III for the two major reaction channels. The apparent activation energies observed for the (110)-(1×2) surface are very similar to, although somewhat smaller than, those observed on the (111) surface—the difference being approximately 1 kcal·mol^{-1} for hydrogenation (i.e., on the order of the experimental uncertainty) and 3.5 kcal·mol^{-1} for hydrogenolysis (cf. Tables II and III). In terms of absolute activities, at a temperature of 450 K, the Ir(110)-(1×2) surface is more active than the Ir(111) surface for both reaction channels by less than a factor of 4. (Note that this value is dependent on the particular site density chosen for the two surfaces.)

As in the case of the Ir(111) surface, when the temperature is increased above approximately 500 K, the production of ethane decreases, while the production of methane increases. Note that the relative selectivity for ethane begins to decrease at a lower temperature on Ir(111), in agreement with results obtained previously concerning propane hydrogenolysis.[25] Again, this change in the selectivity of the hydrogenolysis channel is not accompanied by any change in the apparent reaction kinetics. This is evident in Figure 9, where the total rate of hydrogenolysis is plotted in terms of cyclopropane conversion to C_1 and C_2 products. A least-squares fit of these data gives apparent rate parameters of $k_{app}^{(0)} \simeq 1.3 \times 10^{9\pm1}$ molecules·site^{-1}·s^{-1} and $E_{app} \simeq 22.2 \pm 1$ kcal·mol^{-1}, identical with those given in Table III, which were fit to $T \leq$ 525 K. The decrease in the selectivity for ethane is described best in this case also by an increasing probability of multiple carbon–carbon bond cleavage, due to the decreasing concentration of hydrogen adatoms as the temperature is increased.

The dependence of the specific rates of reaction on the reactant partial pressures has been examined at two different temperatures. Data are shown in Figure 10, for reaction rates measured at 425 K as a function of both the hydrogen and cyclopropane partial pressures, while maintaining a constant partial pressure of the other. Concerning the hydrogenation pathway, the apparent reaction order in P_{HC} is essentially zero, whereas that in P_{H_2} is nearly unity for $P_{H_2} \leq$ 200 Torr and evidently becomes negative for hydrogen partial pressures above 200 Torr. As in the case of the Ir(111) surface, a maximum is observed in the rate of propane production as a function of the hydrogen partial pressure.

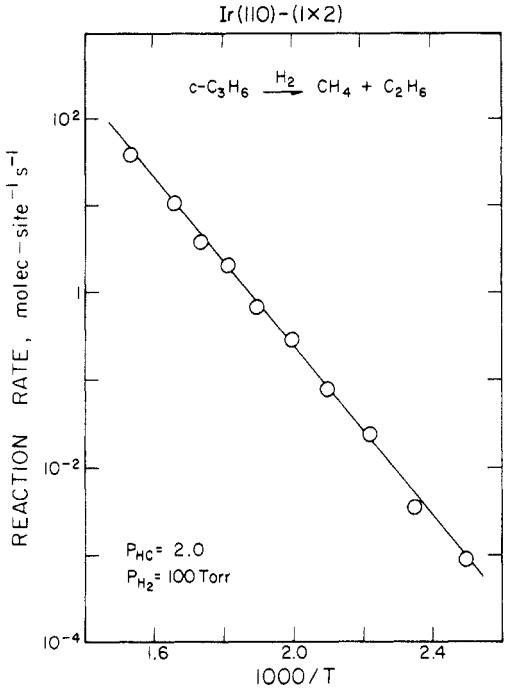

Figure 9. Specific rates of hydrogenolysis of cyclopropane on the Ir-(110)-(1×2) surface, plotted in terms of cyclopropane conversion to methane and ethane. The partial pressure of cyclopropane was 2.0 Torr, and that of hydrogen was 100 Torr.

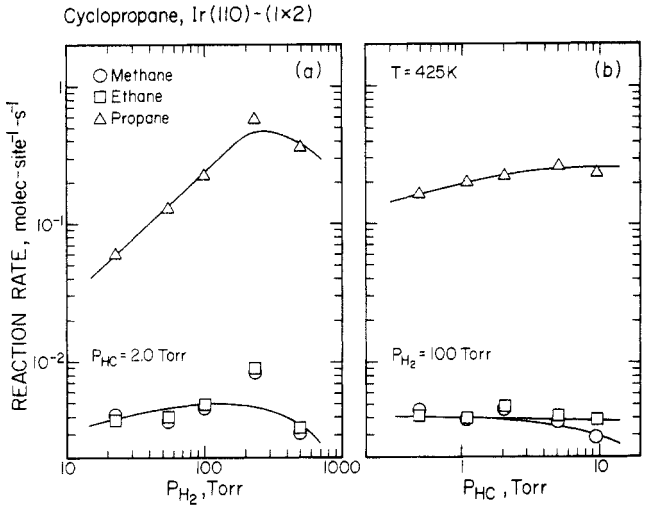

Figure 10. Specific reaction rates for the reaction of cyclopropane and hydrogen on the Ir(110)-(1×2) surface at a temperature of 425 K. (a) The partial pressure of cyclopropane was maintained at 2.0 Torr as the partial pressure of hydrogen was varied. (b) The partial pressure of hydrogen was maintained at 100 Torr as the partial pressure of cyclopropane was varied.

Concerning the hydrogenolysis pathway, the apparent reaction order in both P_{HC} and P_{H_2} is essentially zero, in agreement with the observations on Ir(111). The variation in the specific rates of reaction with respect to the reactant partial pressures differs considerably at the higher temperature of 600 K, as may be seen in Figure 11.

The onset of the selectivity shift observed on the Ir(111) surface at ($P_{H_2}/P_{HC} < 50$) (cf. Figure 5) is apparent on the Ir(110)-(1×2) surface at $P_{H_2}/P_{HC} \leq 10$. As in the case of the Ir(111) surface, the shift is from methane (hydrogenolysis) to propylene (isomerization), as P_{H_2}/P_{HC} is reduced sufficiently. Note, however, that on the Ir(110)-(1×2) surface the selectivity shift from methane to propylene is not complete even at $P_{H_2}/P_{HC} = 10$. That is, these data suggest that the selectivity shift will be complete only upon reducing the hydrogen-to-cyclopropane partial pressure ratio below 10, i.e., experimental conditions not considered here. Postreaction

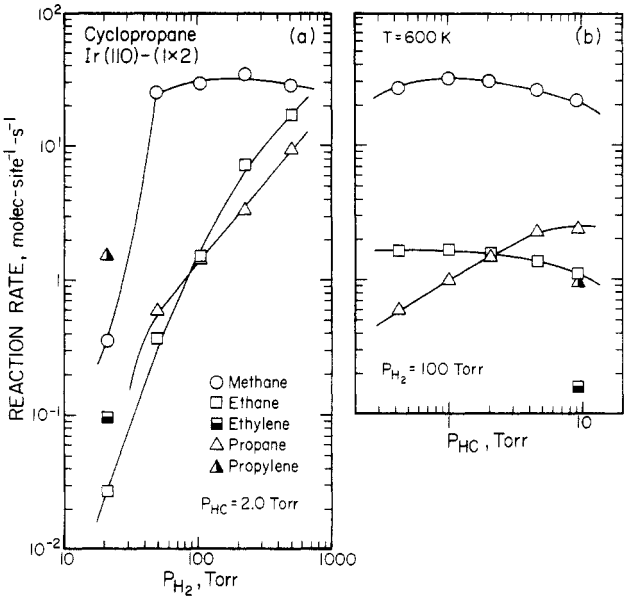

Figure 11. Specific reaction rates for the reaction of cyclopropane and hydrogen on the Ir(110)-(1×2) surface at a temperature of 600 K. (a) The partial pressure of cyclopropane was mainatined at 2.0 Torr as the partial pressure of hydrogen was varied. (b) The partial pressure of hydrogen was maintained at 100 Torr, as the partial pressure of cyclopropane was varied.

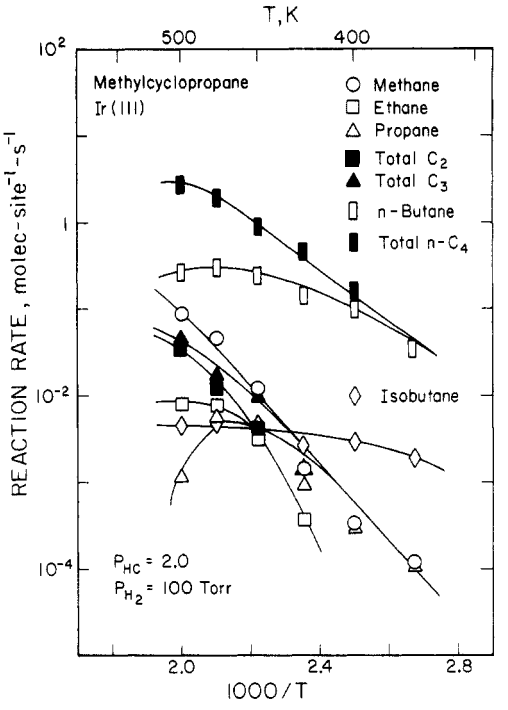

Figure 12. Specific reaction rates for the reaction of methylcyclopropane and hydrogen on the Ir(111) surface. The partial pressure of methylcyclopropane was 2.0 Torr, whereas that of hydrogen was 100 Torr.

surface characterization by Auger electron spectroscopy indicated that for $P_{H_2}/P_{HC} \geq 25$, the fractional coverage of carbon was approximately constant at $\theta_C \simeq 0.59 \pm 0.06$; whereas, for P_{H_2} = 100 Torr and P_{HC} = 9 Torr, the fractional coverage was θ_C = 0.72 and, for P_{H_2} = 21 Torr and P_{HC} = 2 Torr, θ_C = 0.90. The fact that this shift occurs on Ir(110)-(1×2) at lower hydrogen-to-hydrocarbon partial pressure ratios (~10) compared to the Ir(111) surface (~50) indicates that it is more difficult to carburize the (110)-(1×2) surface for this reactant mixture.

B. Methylcyclopropane. 1. Ir(111) Surface. Specific rates of the reaction of methylcyclopropane with hydrogen on the Ir-(111) surface are shown in Figure 12 plotted in an Arrhenius form. Conversions were restricted to below 10%. The coverage of the

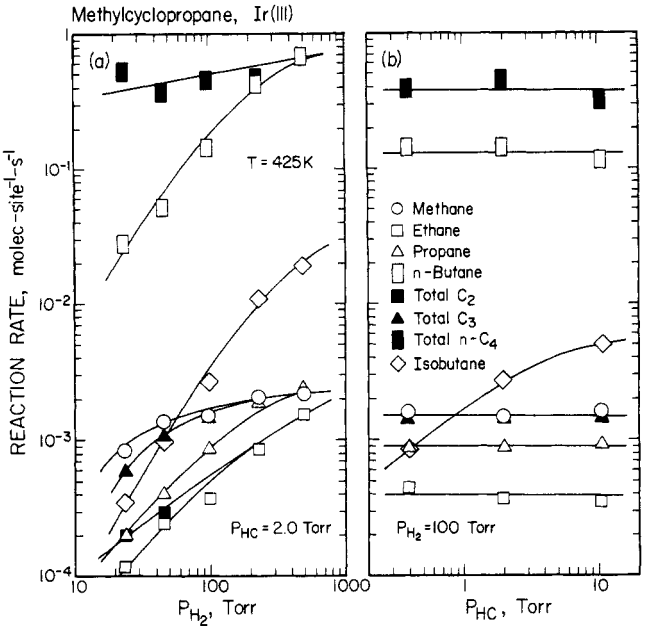

Figure 13. Specific reaction rates for the reaction of methylcyclopropane and hydrogen on the Ir(111) surface at a temperature of 425 K. (a) The partial pressure of methylcyclopropane was maintained at 2.0 Torr as the partial pressure of hydrogen was varied. (b) The partial pressure of hydrogen was maintained at 100 Torr, as the partial pressure of methylcyclopropane was varied.

carbonaceous residue determined via postreaction surface characterization by Auger electron spectroscopy is given in Table I. The coverage of the residue was essentially independent of the reaction conditions considered here (Figure 12) and in text below (Figure 13), and its value is nearly equal to that observed for cyclopropane on this same surface at similar reaction conditions.

As may be seen in Figure 12, a variety of products are observed from the reaction of methylcyclopropane and hydrogen on the Ir(111) surface, namely, methane, ethane, ethylene, propane, propylene, isobutane, *n*-butane, and a mixture of 1- and 2-*n*-butenes. The production of isobutene cannot be ruled out due to overlap with the *n*-butane and 1- and 2-butene chromatographic peaks. However, a conservative estimate places its rate of production below that of isobutane by 1 order of magnitude. The most notable feature of the data shown in Figure 12 is the predominance of the formation of *n*-butane (and 1- and 2-*n*-butenes) from the hydrogenation channel. The major hydrogenation/isomerization channel on the Ir(111) surface is given by

$$c\text{-}C_3H_5CH_3 + H_2 \rightarrow n\text{-}C_4H_{10} \text{ or } n\text{-}C_4H_8$$

whereas the major hydrogenolysis channel is given by

$$c\text{-}C_3H_5CH_3 + 2H_2 \rightarrow CH_4 + C_3H_8$$

The corresponding minor reaction channels involve hydrogenation to isobutane and hydrogenolysis to ethane. Note that, at a temperature of 425 K, conversion of methylcyclopropane to (2 molecules of) ethane is approximately $^1/_{15}$ th of that to methane and propane.

The apparent rate parameters obtained from the data shown in Figure 12 are given in Table II for the two major reaction channels. The parameters for the hydrogenation/isomerization pathway were fit to the total n-C_4 (*n*-butane and 1- and 2-*n*-butene) production, whereas those for hydrogenolysis were fit to the rate of $C_1 + C_3$ production (methane, propane, and propylene). As with cyclopropane, the relative fraction of unsaturated products increases with increasing surface temperature, consistent with a depletion in the steady-state coverage of hydrogen adatoms as the temperature is increased.

It is of interest to compare our experimental observations (e.g., the large *n*-butane-to-isobutane selectivity) to previous work on group VIII metals.[4,8] For example, for similar reactant partial pressures at temperatures near or below 273 K, isobutane has been found to be the major reaction product on both supported platinum (P_{HC} = 50 Torr and P_{H_2} = 50 Torr)[4] and palladium, nickel, and platinum films (P_{HC} = 10 Torr and P_{H_2} = 100 Torr).[8] Similar behavior has been reported for the hydrogenation of *gem*-dimethylcyclopropane by several group VIII metal films and supported catalysts, i.e., the production of neopentane dominates.[9] This apparent disagreement with the work reported here is readily understood by examining the temperature dependence of the selectivity for *n*-butane versus isobutane. In particular,both Bond and Newham[4] and Anderson and Avery[8] have found that, with platinum catalysts, the relative selectivity for *n*-butane increases with temperature, from a value of approximately $^1/_{20}$ at 275 K to a value of nearly unity at 500–525 K. Our experimental data suggest an even greater temperature dependence of the relative selectivity for *n*-butane on iridium. Extrapolating our data shown in Figure 12 to lower temperatures indicates that the rates of *n*-butane and isobutane production should become equivalent at a temperature of approximately 300–325 K. In contrast, the relative selectivity for *n*-butane is approximately 10^3 at 500 K on Ir(111). The fact that the temperature for which the relative selectivity for *n*-butane and isobutane is nearly unity is apparently considerably lower for iridium compared to platinum, could be intrinsic, or could be due to differing reaction conditions between our work and previous investigations (e.g., as discussed below, the dependence of isobutane production on P_{HC} and possibly P_{H_2} differs from that for *n*-butane).

The dependence of the specific rates of reaction on the reactant partial pressures was examined at a temperature of 425 K. These data are shown in Figure 13. The apparent orders in P_{HC} and P_{H_2} are essentially zero with respect to the total production of n-C_4 molecules. Consistent with a decreasing fraction of *n*-butane production with increasing temperature, the apparent order in P_{H_2} for *n*-butane is positive and is essentially equal to unity. The fact that at a similar temperature of 450 K the order in P_{HC} for the hydrogenation/isomerization of cyclopropane is larger (approximately unity) than that for methylcyclopropane (essentially zero) suggests that the adsorbed methylcyclopropane is bound more strongly to the surface and/or formed more easily (i.e., its coverage is nearer the saturation level, and, thus, the order in P_{HC} is nearly zero). With respect to the minor hydrogenation pathway (the production of isobutane), the order in P_{HC} varies between $\sim$1 and $\sim^1/_2$ as P_{HC} is increased, whereas the apparent order in P_{H_2} is approximately $1-1^1/_2$. Thus, the sensitivity (i.e., the apparent orders) of the two hydrogenation/isomerization pathways differ with respect to each other, suggesting that different intermediates may be involved. Concerning the major hydrogenolysis pathway (the formation of methane, propane, and propylene), the order in P_{HC} is zero, whereas that in P_{H_2} is nearly zero and exhibits a small positive value for $P_{H_2} \leq 50$ Torr. These observations are consistent with those for cyclopropane hydrogenolysis on this surface where both orders were essentially zero.

2. Ir(110)-(1×2) Surface. Specific rates of the reaction of methylcyclopropane with hydrogen on the Ir(110)-(1×2) surface are shown in Figure 14, plotted in an Arrhenius form. Conversions were restricted to below 10%. The coverage of the carbonaceous residue following the reaction is given in Table I. The coverage of the residue was nearly independent of the reaction conditions considered here (Figure 14) and in text below (Figure 15), and its value is essentially identical with that observed for methylcyclopropane on the Ir(111) surface.

The products observed on the Ir(110)-(1×2) surface were methane, ethane, propane, isobutane, *n*-butane, and a mixture of 1- and 2-butenes. Again, we estimate that the production of isobutene was smaller than that of isobutane by at least 1 order of magnitude. One additional reaction product, which could not be identified explicitly, was detected. On the basis of the experimental observation that, in the presence of the reaction product mixture and at 300 K, the disappearance of this product was correlated directly with the formation of the parent molecule, methylcyclopropane, a likely candidate is methylenecyclopropane. However, since this identification is in doubt, we shall not discuss the formation of this product further except to note that its rate

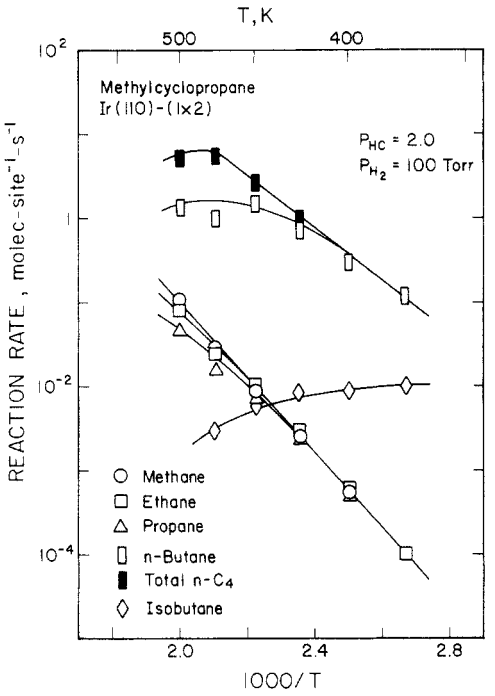

Figure 14. Specific reaction rates for the reaction of methylcyclopropane and hydrogen on the Ir(110)-(1×2) surface. The partial pressure of methylcyclopropane was 2.0 Torr, whereas that of hydrogen was 100 Torr.

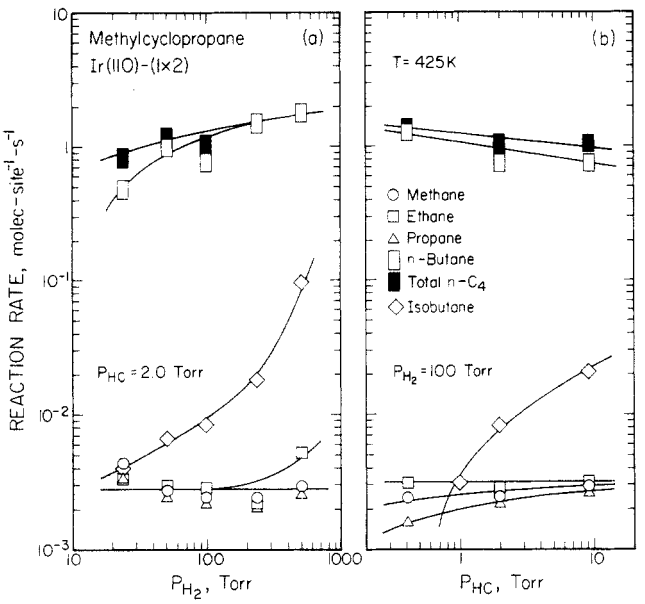

Figure 15. Specific reaction rates for the reaction of methylcyclopropane and hydrogen on the Ir(110)-(1×2) surface at a temperature of 425 K. (a) The partial pressure of methylcyclopropane was maintained at 2.0 Torr as the partial pressure of hydrogen was varied. (b) The partial pressure of hydrogen was maintained at 100 Torr as the partial pressure of methylcyclopropane was varied.

of formation was always much less than that of *n*-butane and the linear butenes.

Unlike the Ir(111) surface, but in agreement with the results for cyclopropane on Ir(110)-(1×2), unsaturated hydrogenolysis products (ethylene and propylene in this case) are not observed on the Ir(110)-(1×2) surface. In addition, the selectivity for *n*-butane begins to decrease at a higher temperature on the (110)-(1×2) surface. For example, the selectivity, n-C_4H_{10}/total n-C_4, is equal to $^1/_2$ at 450 K on Ir(110)-(1×2) compared to 400 K on Ir(111). As may be seen in Figure 14, the dominant hydrogenation/isomerization channel involves the production of *n*-butane and "linear" butenes, as was the case for the Ir(111) surface. However, unlike the Ir(111) surface, there *apparently* is no dominant hydrogenolysis channel on Ir(110)-(1×2). Rather, both the production of $CH_4 + C_3H_8$ and $2C_2H_6$ exhibit similar activities and (possibly fortuitously) similar apparent rate parameters. Recall that the production of CH_4 and C_3H_8 was the dominant hydrogenolysis channel on the Ir(111) surface.

The apparent rate parameters obtained from the data shown in Figure 14 are given in Table III for the two major reaction channels. The parameters for the hydrogenation/isomerization pathway were fit to the total conversion to n-C_4, whereas those for hydrogenolysis were fit to the total rate of conversion to $C_1 + C_2 + C_3$ products. Comparing the two surfaces for the reaction of methylcyclopropane at a temperature of 450 K, the activities for hydrogenolysis are essentially equivalent, whereas the specific rate of hydrogenation/isomerization is greater on the Ir(110)-(1×2) surface by approximately a factor of 4.

The product distribution that is observed for the hydrogenolysis pathway on the Ir(110)-(1×2) surface, i.e., equal amounts of methane, ethane, and propane, can be explained by the following argument. The products from the major reaction channel of hydrogenolysis result from the cleavage of two C–C bonds; i.e., first the ring is opened, and subsequently, a second C–C bond is cleaved in the resulting adsorbed complex, leaving two hydrocarbon "fragments", which are hydrogenated [or desorbed for the unsaturated species on Ir(111)] to the observed products. Considering a random scission of two C–C bonds in the parent methylcyclopropane molecule, restricting C–C bond scission to the ring carbons, there are three possible combinations; two result in the production of $CH_4 + C_3H_8$, and one results in the production of $2C_2H_6$. Thus, for a completely random cleavage of two C–C bonds in the methylcyclopropane ring, the expected product distribution is equal amounts of methane, ethane, and propane, *exactly* what is observed on the Ir(110)-(1×2) surface. The fact that the production of ethane involves cleavage of the two C–C bonds adjacent to the methyl group and that this pathway is apparently a minor channel on Ir(111) (i.e., the surface for which the metal surface atoms are relatively more coordinatively saturated) suggests that steric factors may be involved in the observed hydrogenolysis selectivity.

The dependence of the specific rates of reaction on the reactant partial pressures has been examined at a temperature of 425 K. These data are shown in Figure 15. With respect to the total production of n-C_4 molecules, the apparent order in both P_{H_2} and P_{HC} are essentially zero. Consistent with a decreasing fraction of *n*-butane production with increasing temperature, the apparent order in P_{H_2} for *n*-butane is positive. However, the apparent order in P_{H_2} is smaller on the (110)-(1×2) surface compared to the (111) surface for identical reaction conditions. With respect to the minor hydrogenation pathway (the production of isobutane), the order in P_{HC} is between ~ 1 and $\sim {}^1/_2$, whereas the apparent order in P_{H_2} is approximately $^1/_2$-$1^1/_2$. Again, the differing apparent orders of the two hydrogenation/isomerization pathways suggest that different intermediates may be involved. Concerning the hydrogenolysis pathway, the orders in both P_{HC} and P_{H_2} are essentially zero for all the products observed, suggesting that, in agreement with the apparent reaction kinetics, methane, ethane, and propane are formed from a similar intermediate.

C. Propylene. 1. Ir(111) Surface. Steady-state rates of the reaction of propylene with hydrogen on the Ir(111) surface are shown in Figure 16a, plotted in an Arrhenius form. Conversions were restricted to below 10%. The coverage of the carbonaceous residue corresponding to these reaction conditions is shown in Figure 16b. There is a significant increase in the coverage of the residue for temperatures above approximately 500 K; i.e., for $T \leq 500$ K, $\theta_C \simeq 0.5 \pm 0.1$, whereas, for $T \geq 550$ K, $\theta_C \simeq 1.0 \pm 0.1$. Postreaction thermal desorption of the near-monolayer coverage residue produced spectra similar to spectrum b in Figure 7. Note that, for identical reactant partial pressures, the coverage of the carbonaceous residue was independent of temperature for the reaction of cyclopropane on this surface.

The only reaction products observed on the Ir(111) surface for the reaction conditions considered here were methane, ethane, ethylene, and propane. Two major reaction channels were ob-

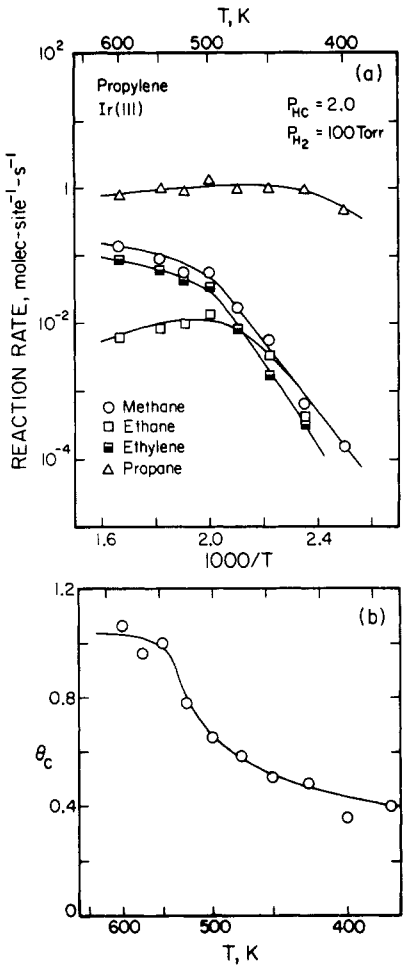

Figure 16. (a) Specific reaction rates for the reaction of propylene and hydrogen on the Ir(111) surface. The partial pressure of propylene was 2.0 Torr, whereas that of hydrogen was 100 Torr. (b) The fractional surface coverage of the carbonaceous residue at the corresponding reaction conditions.

served: hydrogenation to propane and hydrogenolysis to methane and a mixture of ethane and ethylene, the relative selectivity for ethylene increasing with increasing temperature. Compared to cyclopropane on this surface at a temperature of 450 K, the rate of production of propane is approximately a factor of 7 more rapid from propylene, whereas the rate of hydrogenolysis is nearly equivalent for both reactants. The former observation suggests that if cyclopropane and propylene are hydrogenated to propane from a similar intermediate, then the rate of formation of this intermediate from cyclopropane must be less rapid than from propylene.

The specific rate of conversion via both the hydrogenation and hydrogenolysis channels was fit to an Arrhenius expression, and the resulting apparent rate parameters are given in Table II. The apparent activation energy of hydrogenation is nearly zero (−0.2 ± 2 kcal·mol^{-1}), whereas the corresponding apparent preexponential factor is equal to 0.8 × $10^{0\pm1}$ molecules·site^{-1}·s^{-1}. The former value can be compared to that obtained by Mann and Lien[26] for a pumice-supported Ir catalyst where the apparent activation energy was found to be 15 kcal·mol^{-1} for temperatures between 333 and 389 K and reactant partial pressures of P_{HC} = 30 Torr and P_{H_2} = 60 Torr. Unfortunately, these authors made no attempt to measure the surface area of the exposed Ir atoms, and therefore, we cannot compare either the apparent preexponential factors or the specific rates of reaction. On the other hand, the measured rate parameters for propylene hydrogenolysis are similar to those for cyclopropane hydrogenolysis. Unlike cyclopropane, nonlinear Arrhenius behavior is observed in the temperature range examined, $T \simeq$ 400–600 K. The concomitant decrease in the apparent activation energy of hydrogenolysis and increase in the coverage of the carbonaceous residue for temperatures above 500 K suggest that these two events are related.

To obtain supporting evidence for the proposition involving the change in the coverage of the carbonaceous residue, reaction rates were measured as a function of the partial pressure of propylene at a constant partial pressure of hydrogen (100 Torr) and two

(26) Mann, R. S.; Lien, T. R. *J. Catal.* **1969**, *15*, 1.

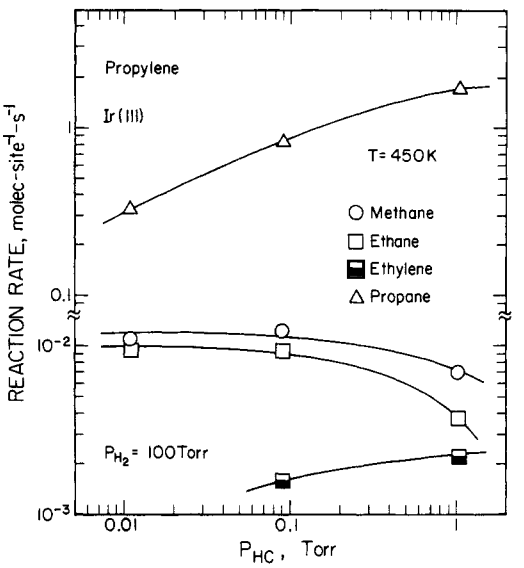

Figure 17. Specific reaction rates for the reaction of propylene and hydrogen on the Ir(111) surface at a temperature of 450 K. The partial pressure of hydrogen was maintained at 100 Torr as the partial pressure of propylene was varied.

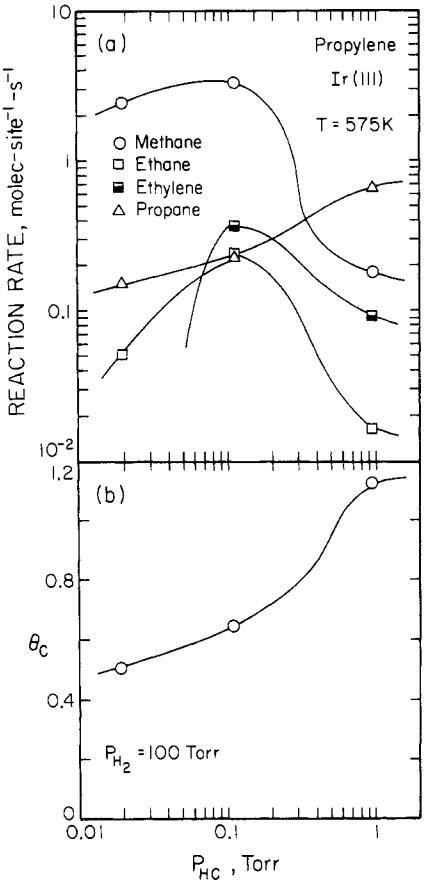

Figure 18. (a) Specific reaction rates for the reaction of propylene and hydrogen on the Ir(111) surface at a temperature of 575 K. The partial pressure of hydrogen was maintained at 100 Torr as the partial pressure of propylene was varied. (b) The fractional coverage of the carbonaceous residue at the corresponding reaction conditions.

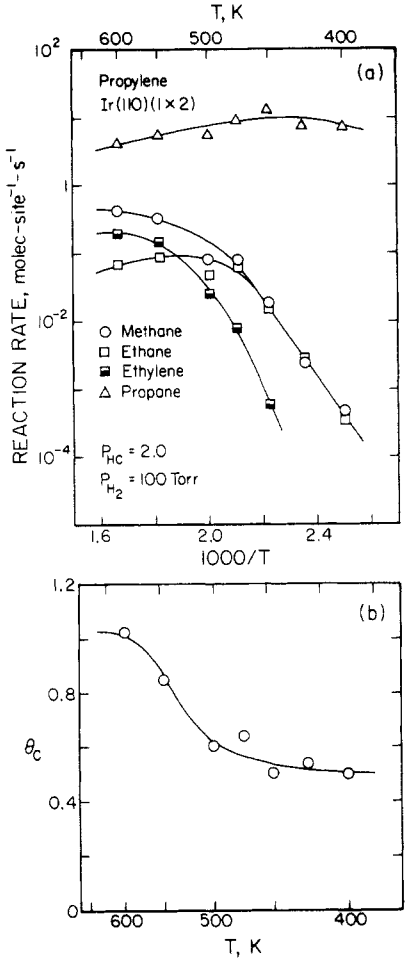

Figure 19. (a) Specific reaction rates for the reaction of propylene and hydrogen on the Ir(110)-(1×2) surface. The partial pressure of propylene was 2.0 Torr, whereas that of hydrogen was 100 Torr. (b) The fractional surface coverage of the carbonaceous residue at the corresponding reaction conditions.

different temperatures. These data are shown in Figures 17 and 18 for temperatures of 450 and 575 K. As may be seen in Figure 17, at a temperature of 450 K, i.e, in the linear Arrhenius region, the apparent order in P_{HC} for the hydrogenolysis channel is essentially zero, whereas that for hydrogenation exhibits a small positive value. The relative rate of ethylene production decreases with decreasing P_{HC}, consistent with a more hydrogen-rich partial pressure ratio. Most importantly, at 450 K, the coverage of the carbonaceous residue is essentially constant at a value of $\theta_C \simeq 0.54 \pm 0.08$.

In contrast, as may be seen from Figure 18, as P_{H_2}/P_{HC} is increased above approximately 200–500 at a temperature of 575 K, there is a shift in both the coverage of the carbonaceous residue and the selectivity. Specifically, as P_{H_2}/P_{HC} is increased, the coverage of the residue is reduced by approximately a factor of 2, whereas the selectivity shifts from hydrogenation (propane) to hydrogenolysis (methane). This behavior, i.e., a dramatic decrease in the hydrogenolysis selectivity on a highly carburized surface, is exactly what was observed for cyclopropane on Ir(111) as shown in Figure 6. The essential difference between these two reactants regarding these phenomenon is that smaller partial pressure ratios P_{HC}/P_{H_2} are sufficient to lead to the highly carburized surface for propylene ($\sim^1/_{200}$) with respect to cyclopropane ($\sim^1/_{50}$). This is presumably due to the relative "ease" of chemisorption of propylene compared to cyclopropane.

2. Ir(110)-(1×2) Surface. Steady-state rates of the reaction of propylene with hydrogen on the Ir(110)-(1×2) surface are shown in Figure 19a, plotted in an Arrhenius form. Conversions were restricted to below 10%. The coverage of the carbonaceous residue corresponding to these reaction conditions is shown in Figure 19b. As in the case of the Ir(111) surface, there is a sharp increase in the coverage of the residue that occurs on Ir(110)-(1×2) near a temperature of 550 K. The fact that this adlayer transformation occurs at a higher temperature on Ir(110)-(1×2) implicates again a superior resistance to self-poisoning and carburization of this surface.

The only reaction products observed for the reaction conditions considered here were methane, ethane, ethylene, and propane. The two major reaction channels were hydrogenation to propane and hydrogenolysis to methane and a mixture of ethane and ethylene, with the relative selectivity for ethylene increasing with increasing temperature. Compared to cyclopropane on this surface at a temperature of 450 K, the rate of production of propane is a factor of approximately 25 more rapid from propylene, whereas the rate of hydrogenolysis is nearly equivalent from both reactants. In comparison to propylene on Ir(111) at a temperature of 450 K, the rate of hydrogenation to propane is a factor of approximately 14 greater on the Ir(110)-(1×2) surface, whereas the rate of hydrogenolysis is more rapid on Ir(110)-(1×2) by approximately a factor of 3.

The specific rate of conversion via both the hydrogenation and hydrogenolysis channels was fit to an Arrhenius expression, and the resulting apparent rate parameters are given in Table III. Both the apparent activation energy (-3.6 ± 2 kcal·mol^{-1} and apparent preexponential factor ($0.2 \times 10^{0\pm1}$ molecules·site^{-1}·s^{-1}) of hydrogenation and similar to those found on the Ir(111) surface. The rate parameters for propylene hydrogenolysis compare well to those observed for cyclopropane hydrogenolysis on Ir(110)-(1×2) and Ir(111) for propylene hydrogenolysis on Ir(111). In addition, as with the Ir(111) surface, the nonlinear Arrhenius behavior apparent above 500 K can be attributed to the increase in the coverage of the carbonaceous residue.

IV. Discussion

The hydrogenation of cyclopropane to propane has been reported to be slightly "structure-sensitive"[27] on both supported nickel[12] and platinum,[11] in agreement with the results reported here for two different single-crystalline surfaces of iridium. In particular, the specific activity (for both hydrogenation and hydrogenolysis) of the Ir(110)-(1×2) surface is greater than that of the Ir(111) surface, the ratio varying between a factor of 2 and 10. This difference in the specific activities is on the order of those reported previously for the supported nickel[12] and platinum[11] catalysts of varying particle size, where larger specific activities were found for the smaller particles. However, it is significantly less than that reported for the single-crystalline (111) and (100) surfaces of nickel,[13] where, under similar reaction conditions, a difference of greater than 1 order of magnitude was found.

With respect to the experimental measurements reported here, the previous results on the supported nickel catalysts of varying metallic particle size are most suggestive. A specific activity (of hydrogenation *and* hydrogenolysis) was reported for catalysts with an average crystallite diameter of 12 Å that was a factor of 3 greater than that observed for much larger crystallites with average diameters greater than 50 Å. Previous work concerning the hydrogenolysis of *n*-butane on these same Ir(110)-(1×2) and Ir(111) surfaces[28] led us to compare the results for the iridium single crystals to supported iridium catalysts of varying particle size.[29] In making this comparison, "effective particle sizes" were computed for the single-crystalline surfaces by utilizing the ratio of the number of edge (C_7) atoms to the number of (111) face (C_9) atoms as the appropriate criterion (cf. Figure 1). Depending on the particular polyhedron chosen for the crystallite shape, the effective particle sizes are 13–24 Å for the Ir(110)-(1×2) surface and 81–166 Å for the Ir(111) surface. (Utilizing the Ni–Ni lattice spacing, we find that the effective particle size for the Ir-(110)-(1×2) surface is 12–22 Å.) Thus, the results presented here [implicating a greater specific activity for the Ir(110)-(1×2) surface] and those obtained on supported nickel catalysts [im-

(27) Boudart, M. *Adv. Catal.* **1969**, *20*, 153.
(28) Engstrom, J. R.; Goodman, D. W.; Weinberg, W. H. *J. Am. Chem. Soc.* **1986**, *108*, 4653.
(29) Foger, K.; Anderson, J. R. *J. Catal.* **1979**, *59*, 325.

plicating a greater specific activity for crystallites with average diameters of 12 Å] can be reconciled if the low-coordination-number (C_7) atoms possess an activity for this reaction that is intrinsically greater than that possessed by the more highly coordinated (111) face (C_9) atoms. If this is the case, the intrinsic activity difference could be related to differences in the local electronic density between C_7 and C_9 atoms.

The results obtained for cyclopropane on the Ir(111) surface suggested that propane and propylene are formed from a common intermediate (cf. Figures 2 and 4). Although we have presented here only measurements of the reaction kinetics, i.e., direct spectroscopic evidence is lacking, we feel compelled to speculate as to possible reaction intermediates. For example, a reasonable structure for this intermediate is a 1,2-di-σ-bound C_3H_6(a) species. However, the observation of a positive order in P_{H_2} for the total rate of C_3 (propane and propylene) production can be rationalized if the common intermediate is more dehydrogenated than propylene, e.g., a C_3H_5(a) species. One species that is consistent with the C_3H_5 stoichiometry is a π-allyl. Addition of a hydrogen atom at the 1 or 3 positions of a π-allyl would produce either the aforementioned 1,2 di-σ-bonded C_3H_6 or a π-bonded propylene. Additional hydrogenation would lead to propane, whereas desorption would lead to propylene, consistent with the observations on the Ir(111) surface. This interpretation is obviously not unique. However, there are precedents from organometallic chemistry that involve the reaction of transition-metal homogeneous complexes with cyclopropane, which lead to the coordination of a π-allyl ligand, including an Ir(I) complex.[30]

The hydrogenolysis of cyclopropane to methane and ethane [and ethylene on Ir(111)] was found to be qualitatively different from the hydrogenolysis of propane. For example, over the entire range of temperatures considered on both surfaces (cf. Figures 3 and 9), there was no observable variation in the apparent reaction kinetics. This was corroborated by the lack of any significant variation in the apparent reaction "orders", the order in both P_{HC} and P_{H_2} being essentially zero. These observations can be interpreted by a reaction mechanism involving relatively facile formation of the adsorbed intermediate (i.e., the step that "opens" the ring), with the rate-limiting step being (secondary) C–C bond cleavage in the adsorbed intermediate [i.e., subsequent hydrogenation, desorption, and additional hydrogenolysis (i.e., $C_2 \rightarrow 2C_1$) are rapid with respect to C–C bond cleavage in the adsorbed intermediate]. The major difference between this mechanism and that proposed previously for propane (alkane) hydrogenolysis[25] is that formation of the intermediate is both facile and irreversible for cyclopropane.

A reasonable reaction for the first (facile) step is the oxidative addition of cyclopropane to the Ir surface (i.e., ring-opening), forming a "1,3" di-σ-bonded C_3H_6 species. A likely candidate for the adsorbed species is a metallacycle butane since, for example, the most common route to (synthesis of) metallacycle butanes in organometallic chemistry is the addition of cyclopropane to complexes of transition metals in low formal oxidation states.[31] Of particular interest here, the fragmentation of metallacycle butane ligands in homogeneous transition-metal complexes to form olefins and carbenes is well-known[32] and, thus, provides an established mechanism for hydrogenolysis. The observation of the production of ethylene from the hydrogenolysis channel on Ir(111) suggests that a metallacycle butane is the dominant intermediate (and mechanism) for hydrogenolysis. The absence of the production of ethylene on Ir(110)-(1×2) (excepting the "severe" reaction conditions of Figure 11) does not necessarily suggest a different mechanism. Rather, it may be a manifestation of a greater specific activity for the hydrogenation of ethylene possessed by the Ir(110)-(1×2) surface.

The most significant result concerning the reaction of methylcyclopropane on these two iridium surfaces is the dominance of the production of *n*-butane (and 1- and 2-butenes) from the hydrogenation (isomerization) channel. This result can be interpreted qualitatively, as discussed in Section III.B.1, by considering two parallel reaction channels, with the production of *n*-butane exhibiting a higher apparent activation energy and preexponential factor. In this picture, the C_2–C_3 bond of methylcyclopropane is cleaved at low temperatures. This interpretation, of course, does not explain *why* *n*-butane production dominates at high temperatures.

Clues as to the nature of the reaction mechanism that leads to the production of *n*-butane can be obtained by examining the specific cases for which a high selectivity for *n*-butane has been observed. For example, Anderson and Avery[8] observed a product ratio n-C_4H_{10}:i-C_4H_{10} of 2:1 from the reaction of methylcyclopropane with deuterium on tungsten films at temperatures of 290–310 K (P_{HC} = 10 Torr and P_{H_2} = 100 Torr). Of particular interest, under identical reaction conditions, the major products were *deuteriomethylcyclopropanes*, where the exchange with the parent methylcyclopropane was limited to the "ring hydrogens". On the other hand, under similar reaction conditions on palladium, nickel, and platinum films (T = 210–270 K and identical P_{HC} and P_{H_2}), the product ratio n-C_4H_{10}:i-C_4H_{10} was always less than 1:10 and no exchange products were detected. Chevreau and Gault[9] have reported similar results concerning the reactions of *gem*-dialkylcyclopropanes. For example, on tungsten films, the major reaction product from 1,1-dimethylcyclopropane was isopentane, and its relative rate of production (selectivity) increased with temperature; e.g., isopentane represented 80% of the products at 275 K and 98% at 575 K. These results suggest that, in cases for which C–H bond activation (apparently) precedes C–C bond activation,[33] the ring opens adjacent to the most subsituted carbon atom.

Gault and co-workers[10] have also examined the reaction of 1,2-*cis*- and 1,2-*trans*-dimethylcyclopropanes with hydrogen on platinum, nickel, and palladium films at temperatures between 275 and 325 K (P_{HC} = 5 Torr and P_{H_2} = 60 Torr). In all cases, isopentane was the major reaction product. However, *n*-pentane was detected, and its relative rate of production increased with increasing temperature. Most importantly, on platinum films the relative selectivity for *n*-pentane was approximately 20% from the cis isomer, whereas it was only 1% from the trans isomer. These results may be interpreted, as they have been recently,[35] by invoking a "flat" adsorbed intermediate (or transition state), i.e., the plane of the ring being parallel to the metal surface, for the production of *n*-pentane, and "edge-on" dissociative adsorption [essentially that described above for metallacycle butane formation[31]] for the production of isopentane. It is of interest to note that both of the mechanisms discussed here for the production of *n*-butane from methylcyclopropane—C–H bond activation preceding (or concomitant with) C–C bond activation or a "flat" adsorbed intermediate—would appear to suggest the (eventual) participation of a π-allyl species in the hydrogenation channel.[36]

The selectivity difference observed between Ir(111) and Ir(110)-(1×2) for the hydrogenolysis of methylcyclopropane can be explained on the basis of structural considerations. The presence of propylene from the major (hydrogenolysis) reaction channel on Ir(111) suggests, as was the case for cyclopropane,

(30) Tulip, T. M.; Ibers, J. A. *J. Am. Chem. Soc.* **1979**, *101*, 4201.
(31) Puddephatt, R. J. *Coord. Chem. Rev.* **1980**, *33*, 149.
(32) See, e.g.: Straus, D. A.; Grubbs, R. H. *Organometallics* **1982**, *1*, 1658.
(33) C–H bond activation of cyclopropanes has been observed to precede C–C bond activation (i.e., ring-opening) with transition-metal homogeneous complexes.[34]
(34) See, e.g.: Periana, R. A.; Bergman, R. G. *J. Am. Chem. Soc.* **1984**, *106*, 7272.
(35) Zsigmond, A. G.; Notheisz, F.; Bartók, M. *Proceedings of the 5th International Symposium on Catalysis*, Varna, Bulgaria, 1983; Vol. 1, p 345.
(36) It is of interest to note that, on supported platinum catalysts,[37] the major ring-opening products from the reaction of hydrogen (100 Torr) and methylenecyclopropane (50 Torr) have been found to be *n*-butane (at T = 290 K) and linear butenes (at T = 373 K). Thus, the high selectivity observed here for the production of *n*-butene and linear butenes from the reaction of methylcyclopropane and the aforementioned (see section III.B.2) possible production of methylenecyclopropane would appear to be consistent with the suggestion that C–H (as well as C–C) bond activation is important in the hydrogenation channel.
(37) Bond, G. C.; Newham, J. *Trans. Faraday Soc.* **1960**, *56*, 1851.

the involvement of a metallacycle butane in the hydrogenolysis channel. If the pathway to this intermediate involves an "edge complex," as has been discussed elsewhere,[31] then the presence of the methyl group may provide a steric limitation as to the activation of the C_1–C_2 bond. Since the presence of ethane (or ethylene) from the hydrogenolysis of methylcyclopropane can only be described (for this mechanism) by the fragmentation of a metallacycle butane that has been formed from the activation of the C_1–C_2 bond, the selectivity observed for the hydrogenolysis channel should be decisive in determining if a steric limitation exists on either surface. In fact, the selectivity is quite different for the major reaction channels on the two surfaces—the product distribution is $CH_4 + C_3H_8$ on Ir(111), whereas it is $CH_4 + C_2H_6 + C_3H_8$ on Ir(110)-(1×2). This result can be interpreted readily by considering the stereochemistry of the two surfaces. In particular, an edge complex involving the C_1–C_2 bond of methylcyclopropane and the C_9 atoms of the Ir(111) surface is precluded by the presence of the methyl group, whereas an edge complex involving the C_1–C_2 bond may be formed with the low-coordination-number C_7 atoms, which are present (in significant concentrations) only on the Ir(110)-(1×2) surface. Consequently, the absence of ethane in the major hydrogenolysis channel on Ir(111) can be explained purely on a stereochemical basis. It is important to note that, as evidenced by the dominant production of *n*-butane, activation of the C_1–C_2 bond *does* occur on Ir(111) for the hydrogenation/isomerization channel, the selectivity for hydrogenation of methylcyclopropane being essentially identical with that on the Ir(110)-(1×2) surface. This observation implies that on both surfaces the production of *n*-butane from methylcyclopropane does not involve an edge complex; rather, possibly the flat intermediate suggested above.

Finally, comments must be made concerning the apparent superior ability of the Ir(110)-(1×2) surface to hydrogenate surface carbon and/or hydrocarbon fragments. The experimental evidence for this superior ability includes the following observations:

(i) Unsaturated products (ethylene and propylene) are not observed from the reaction of cyclopropane and hydrogen on Ir(110)-(1×2) at the standard reactant partial pressures (P_{HC} = 2.0 Torr and P_{H_2} = 100 Torr).

(ii) Higher partial pressure ratios, P_{HC}/P_{H_2}, are necessary to carburize the Ir(110)-(1×2) surface from the reaction of cyclopropane and hydrogen.

(iii) Unsaturated hydrogenolysis products (ethylene and propylene) are not observed from the reaction of methylcyclopropane and hydrogen on Ir(110)-(1×2) at the standard reactant partial pressures (P_{HC} = 2.0 Torr and P_{H_2} = 100 Torr). In addition, for identical reaction conditions, the selectivity for *n*-butane (with respect to total *n*-C_4) is greater on Ir(110)-(1×2).

(iv) The specific rate of hydrogenation of propylene is greater on the Ir(110)-(1×2) surface.

(v) The selectivity for ethylene from the reaction of propylene and hydrogen is greater on Ir(111). In addition, higher temperatures are necessary to carburize the Ir(110)-(1×2) surface for this reaction.

Independent measurements of the adsorption and desorption kinetics of hydrogen on the *clean* (111) and (110)-(1×2) surfaces of iridium have verified the presence of a higher binding energy adstate on the (110)-(1×2) surface.[23,24] Thus, it might be expected that the hydrogen adatom concentration will be greater on the Ir(110)-(1×2) surface during the reactions reported here, and this could explain a greater rate of hydrogenation on the Ir(110)-(1×2) surface. It must be noted, however, that if one utilizes the clean surface values that describe the kinetics of adsorption and desorption,[23,24] the coverage of hydrogen [with respect to vacant sites[25]] is calculated to be near the saturation level on *both* surfaces. On the other hand, if both surfaces are "saturated" with hydrogen adatoms, it is difficult to reconcile a positive reaction order in P_{H_2}, which is observed for the reaction c-$C_3H_6 + H_2 \rightarrow C_3H_8$ on both Ir(111) (cf. Figures 4 and 5) and on Ir(110)-(1×2) at 600 K (cf. Figure 11). It is entirely possible that the carbonaceous residue (near a coverage of $\theta_C \simeq 0.5$ at the standard reactant partial pressures) may perturb the binding energy of the hydrogen adatoms such that the hydrogen coverages are not near saturation, and, thus, do differ significantly. Alternatively, other more subtle effects may be involved. For example, it is also possible that the Ir(110)-(1×2) surface binds olefins more strongly than the Ir(111) surface such that the rate of desorption cannot compete with that of hydrogenation on the Ir(110)-(1×2) surface.

Clues to the plausibility of the preceding arguments would be aided, for example, by a more complete study of the hydrogenation of propylene over the two surfaces, e.g., the apparent reaction orders in both P_{HC} and P_{H_2}. In particular, on Ir(111) and at T = 450 K, the reaction order in P_{HC} is clearly positive, which suggests that the coverage of the adsorbed reaction intermediate [presumably 1,2-di-σ-bonded C_3H_6(a)] is not at this saturation value. Thus, the binding energy (heat of adsorption) of the C_3H_6(a) species will manifest itself in the apparent reaction kinetics. If we apply the Horiuti–Polanyi mechanism,[38] which describes the hydrogenation of ethylene, to the hydrogenation of propylene, the apparent activation energy will be given by $E_{app} = E_r + \alpha\Delta H_{H_2} + \beta\Delta H_{HC}$, where E_r is the activation energy for the hydrogenation reaction [e.g. C_3H_7(a) + H(a) $\rightarrow$ C_3H_8(g)], α is the order in P_{H_2}, ΔH_{H_2} is the (negative) heat of adsorption of hydrogen, β is the order in P_{HC}, and ΔH_{HC} is the (negative) heat of adsorption of propylene. Thus, depending on the apparent reaction orders, the apparent activation energy can be negative, such as is observed here on Ir(110)-(1×2) (cf. Figure 19). Unfortunately, in the absence of a more complete data set, it is impossible to identify explicitly the cause for the different specific activities and apparent reaction kinetics (cf. Tables II and III) for the hydrogenation of propylene on the two iridium surfaces examined here.

V. Conclusions

The hydrogenation, isomerization, and hydrogenolysis of cyclopropane, methylcyclopropane, and propylene have been examined on the Ir(111) and Ir(110)-(1×2) surfaces. These two surfaces were chosen in order to evaluate the role of low-coordination-number metal surface atoms in these reactions. The (110)-(1×2) surface was found to be more active than the (111) surface for both the hydrogenation (to propane) and the hydrogenolysis (to methane and ethane) of cyclopropane. A comparison of these results to those reported previously for both supported nickel[12] and platinum[11] catalysts suggests that this activity difference could be due to a greater intrinsic activity of the low-coordination-number (C_7) metal surface atoms for these reactions.

Postreaction surface analysis revealed the presence of a carbonaceous residue, the coverage of which was found to vary with both the reaction conditions and the particular reaction (i.e., reactant) examined. For cyclopropane at the "standard" reactant partial pressures (P_{HC} = 2.0 Torr and P_{H_2} = 100 Torr) and for temperatures between 400 and 600 K, the fractional coverage of the residue was essentially constant ($\theta_C \simeq 0.5$) on both surfaces. However, for temperatures near 575–600 K, as the partial pressure ratio P_{HC}/P_{H_2} was increased sufficiently [>50 on Ir(111), >10 on Ir(110)-(1×2)], the fractional coverage of the residue increased dramatically, approaching one monolayer. Concomitant with the transformation in the coverage of the carbonaceous residue, the selectivity of the reaction of cyclopropane and hydrogen was found to shift from methane (hydrogenolysis) to propylene (isomerization). We have associated this selectivity shift with a perturbation in the catalytic properties of the metal surface by the high-coverage carbonaceous residue. This perturbation results in either (or possibly both) a reduction in the binding energy or a change in the structure of the adsorbed reaction intermediate associated with hydrogenolysis. Consequently, the selectivity is shifted to the (relatively facile) isomerization reaction.

On the Ir(111) surface, propane and propylene are formed from a common intermediate from the reaction of cyclopropane. Possible structures for the reaction intermediate have been discussed; one such possible intermediate is an π-allyl. Although

(38) Horiuti, J.; Polanyi, M. *Trans. Faraday Soc.* **1934**, *30*, 1164.

propylene is not observed for the same reaction conditions on Ir(110)-(1×2), there is no evidence to suggest that a different intermediate is involved [i.e., there is ample evidence that the (110)-(1×2) surface possesses a greater specific activity for hydrogenation reactions]. The hydrogenolysis of cyclopropane was found to be qualitatively different from the hydrogenolysis of propane.[25] In particular, for cyclopropane on both surfaces, there was no variation in the apparent reaction kinetics over the entire temperature range investigated ($T \simeq 400$–600 K). This difference between cyclopropane and propane is due to the irreversibility of forming the adsorbed intermediate from cyclopropane. The observation of the production of ethylene on Ir(111) from the hydrogenolysis channel, coupled with precedents from organometallic chemistry,[31,32] suggests that the adsorbed intermediate is a mononuclear metallacycle butane. The lack of the observation of ethylene on Ir(110)-(1×2) does not exclude the possibility that this mechanism is dominant on both surfaces.

The hydrogenation of methylcyclopropane on both the Ir(111) and Ir(110)-(1×2) surfaces was found to be dominated by the production of *n*-butane for the reaction conditions considered here. This result was interpreted qualitatively by invoking parallel reaction mechanisms for the production of *n*-butane and isobutane, with the *n*-butane channel exhibiting a higher apparent activation energy and, thus, dominating at the relatively high temperatures. Different apparent reaction orders in P_{HC} and P_{H_2} for the production of *n*-butane compared to isobutane suggest that different intermediates (mechanisms) may be involved for the two hydrogenation pathways. We suggest that a π-allylic species may be involved in the reaction channel that produces *n*-butane and "linear" butenes, whereas a 1,3 di-σ-bonded intermediate is probably associated with the production of isobutane. The hydrogenolysis of methylcyclopropane was found to be similar to that found for cyclopropane on both surfaces. The observation of the production of propylene on the Ir(111) surface is consistent with the participation of a metallacycle butane in the hydrogenolysis channel. The selectivity difference observed between the two surfaces for the major hydrogenolysis channels would appear to support this mechanism. In particular, the absence of ethane in the major hydrogenolysis channel on the Ir(111) surface can be explained on a stereochemical basis if metallacycle butane formation proceeds through an edge complex[31] i.e., the presence of the methyl group prevents activation of the C_1–C_2 bond in methylcyclopropane by the coordinatively more saturated C_3 atoms of the Ir(111) surface.

Finally, the Ir(110)-(1×2) surface was found to possess a greater specific activity with respect to the Ir(111) surface for the hydrogenation of propylene. This observation, coupled with a number of others, implies a greater specific activity of the Ir(110)-(1×2) surface for hydrogenation reactions. One simple explanation for these observations is that the hydrogen adatom concentration is greater on the Ir(110)-(1×2) surface due to the presence of a previously identified,[23,24] higher binding energy adstate for hydrogen on this surface.

Acknowledgment. This work was performed at Sandia National Laboratories and supported by the U.S. Department of Energy under Contract DE-AC04-76DP00789. We acknowledge the partial support of the Office of Basic Energy Sciences, Division of Chemical Science (D.W.G.), and National Science Foundation Grant No. CHE-8617826 (W.H.W.).

Registry No. Ir, 7439-88-5; cyclopropane, 75-19-4; methylcyclopropane, 594-11-6; propylene, 115-07-1.

Laser-Induced Activation of Methane at Oxide Surfaces: A Probe of Radical–Surface Interactions

Basseera A. Sayyed and Peter C. Stair*

Department of Chemistry, Northwestern University, Evanston, Illinois 60208 *(Received: March 17, 1989; In Final Form: June 12, 1989)*

C–H bond activation was studied via pulsed laser irradiation of oxides in a methane atmosphere. Carbon monoxide was the major product observed at low power densities and room temperature. Significant amounts of C_2 products, ethane, ethylene, and acetylene were formed. CO, C_2H_6, C_2H_4, and C_2H_2 are assigned as primary products of the reaction. Laser-induced methane activation produces $^{\bullet}CH_3$ and $:CH_2$ radical species in the gas phase via a plasma mechanism and is utilized as a tool to study radical–oxide surface interactions. These reactions are surface sensitive as evidenced by the changes in conversion and product selectivity as a function of oxide pretreatment and oxides used.

Introduction

Methane activation is a subject of considerable scientific and practical interest. This is mainly due to the large abundance of methane, a major component of natural gas present in remote areas of the world, and the enormous economic gains possible in converting it to easily transportable liquid fuels. In general, thermal routes to methane activation have been inefficient due to the endothermicity of the process.[1,2] Commercial processes presently used to convert methane to synthetic crude and gasoline distillate usually involve steam reforming to produce synthesis gas as an intermediate step.[2,3] The substantial capital investments required to implement this process have motivated research into the possibility of more economical, direct methane conversion processes. Oxidative coupling of methane over oxide catalysts is one approach currently being explored.

Keller and Bhasin[4] studied the catalytic oxidative coupling of methane to C_2 compounds over γ-Al_2O_3 supported metal oxides. Methane and oxygen were fed into the reactor cyclically to minimize competing gas-phase noncatalyzed reactions. The metal oxide catalyst undergoes a Mars–van Krevelen type mechanism[5] with the lattice oxygen participating in a redox cycle. Methyl radicals produced at the oxide surface as a result of hydrogen abstraction react to form C_2 compounds. At present, it is not entirely clear whether this reaction occurs primarily in the gas phase or at the oxide surface.

Sofranko et al. found that cyclic redox and methane/oxygen cofeed reactions over Mn/SiO_2 catalysts resulted in comparable

(1) Chamberlain, D. S.; Bloom, E. B. *Ind. Eng. Chem.* **1929**, *21*, 945.
(2) Sofranko, J. A.; Leonard, J. J.; Jones, C. A. *J. Catal.* **1987**, *103*, 302.
(3) Jones, C. A.; Leonard, J. J.; Sofranko, J. A. *Energy Fuels* **1987**, *1*, 12.
(4) Keller, G. E.; Bhasin, M. M. *J. Catal.* **1982**, *73*, 9.
(5) Mars, P.; van Krevelen, D. W. *Chem. Eng. Sci. Suppl.* **1954**, *3*, 41.

0022-3654/90/2094-0409$02.50/0